Characterization of gonadotropins and their receptors in a chondrichthyan, Scyliorhinus canicula, fills a gap in the understanding of their coevolution

Fabian Jeanne, Stanislas Pilet, Danièle Klett, Yves Combarnous, Benoît Bernay, Sylvie Dufour, Pascal Favrel, Pascal Sourdaine

General and Comparative Endocrinology 358 (2024) 114614

Contents lists available at ScienceDirect

General and Comparative Endocrinology

journal homepage: www.elsevier.com/locate/ygcen

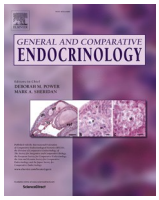

Characterization of gonadotropins and their receptors in a chondrichthyan, *Scyliorhinus canicula*, fills a gap in the understanding of their coevolution

Fabian Jeanne [a], Stanislas Pilet [a], Danièle Klett [b], Yves Combarnous [b], Benoît Bernay [c], Sylvie Dufour [a], Pascal Favrel [a], Pascal Sourdaine [a,*]

[a] Université de Caen Normandie, MNHN, SU, UA, CNRS, IRD, Laboratoire de Biologie des Organismes et Ecosystèmes Aquatiques (BOREA), UMR 8067, 14032 Caen cedex 5, France
[b] INRAE, CNRS, UMR Physiologie de la Reproduction & des Comportements, 37380 Nouzilly, France
[c] Université de Caen Normandie - Plateforme PROTEOGEN, US EMerode, 14032 Caen cedex 5, France

ARTICLE INFO

Keywords:
Gonadotropins
Gonadotropin receptors
Follicle-stimulating hormone
Luteinizing hormone
Spermatogenesis
Chondrichthyes
Elasmobranchs
Shark
Evolution
Testis
Epididymis

ABSTRACT

In Gnathostomes, reproduction is mainly controlled by the hypothalamic-pituitary–gonadal (HPG) axis, with the involvement of the pituitary gonadotropic hormones (GTH), follicle-stimulating hormone (FSH) and luteinizing hormone (LH), which activate their cognate receptors, FSHR and LHR, expressed in gonads. Each GTH consists of a common α subunit and of a specific FSHβ or LHβ subunit. Chondrichthyes (holocephalans and elasmobranchs) is a sister group of bony vertebrates. This position is highly favorable for the understanding of the evolution of endocrine regulations of reproduction among gnathostomes. Surprisingly, the characterization of gonadotropins and their receptors is still limited in chondrichthyes. In the present study, GTH and GTHR sequences have been identified from several chondrichthyan genomes, and their primary structures were analyzed relative to human orthologs. 3D models of GTH/GTHR interaction were built, highlighting the importance of the receptor hinge region for ligand recognition. Functional hormone-receptor interactions have been studied in HEK cells using the small-spotted catshark (*Scyliorhinus canicula*) recombinant proteins and showed that LHR was specifically activated by LH whereas FSHR was activated by both FSH and LH. Expression profiles of GTHs and their receptors were explored by real-time PCR, *in situ* hybridization and immunohistochemistry during spermatogenesis, along the male genital tract and other tissues, as well as in some female tissues for comparison. Tissue-expression analyses showed that the highest levels were observed for *fshr* transcripts in testis and ovary and for *lhr* in specific extragonadal tissues. The two receptors were expressed at all stages of spermatogenesis by both germ cells and somatic cells, including undifferentiated spermatogonia, spermatocytes, spermatids, somatic precursors and Sertoli cells; differentiated Leydig cells being absent in the testis of *S. canicula*. Receptors were also expressed by the lymphomyeloid epigonal tissue and the testicular tubules. These results, suggest a wide range of gonadotropin-regulated functions in Elasmobranchs, as well as functional redundancy during spermatogenesis. These extended functions are discussed in an evolutionary context in which the specificity of gonadotropin signaling must have contributed to the evolution of gonadal cells' morphology and function.

1. Introduction

Gonadotropic hormones (GTH) and their receptors (GTHR) of the hypothalamic-pituitary–gonadal (HPG) axis play a crucial role in the endocrine regulation of reproduction (Campbell, 2004). GTHs belong to the glycoprotein hormones (GPHs) family, also including thyroid-stimulating hormone (TSH). They comprise a common α-subunit (CGA) and a specific β-subunit (LHβ, FSHβ or TSHβ) that are non-covalently associated, and interact with their cognate leucine-rich repeat G protein-coupled receptors (LGRs) (Hsueh and Feng, 2020). They are classic examples of the coevolution of ligand-receptor interaction complexes following their ancient evolutionary origin (Kudo et al., 2000). In fact, an ancestral form of LGRs has been identified in Placozoa and its subsequent evolution has given rise to three types of receptors, including subtype A LGRs found as early as in cnidaria, which could be considered the GPH receptor (GPHR) ancestral form (Van Hiel

* Corresponding author.
E-mail address: pascal.sourdaine@unicaen.fr (P. Sourdaine).

https://doi.org/10.1016/j.ygcen.2024.114614
Received 4 July 2024; Received in revised form 18 September 2024; Accepted 22 September 2024
Available online 24 September 2024

et al., 2012). In the same way, an early tandem duplication of a single ancestral gene encoding a cystine knot protein led to the first two GPHs subunit genes, *gpa2* and *gpb5* identified in ecdysozoans (Kudo et al., 2000; Sudo et al., 2005) and lophotrochozoans (Heyland et al., 2012) and which can be considered the ancestors of the α- and β-subunits families. In the oldest lineage of vertebrates (cyclostomata), GPA2 and GPB5 were identified at the same time as the ancestral GpHβ has emerged concomitantly (at the evolution scale) with a first diversification of GPHRs, as shown by the identification of GpHRI and GpHRII, in the lamprey (Hausken et al., 2018; Hsueh and He, 2018). Furthermore, the recombinant heterodimer GPA2/GPB5 could activate the two receptors while GPA2/GpHβ activated only GpHRI (Hausken et al., 2018). Then, the two differentiated GTHs corresponding to the follicle stimulating hormone (FSH) and luteinizing hormone (LH), with their respective receptors, FSHR and LHR, would have emerged in chondrichthyes, before their divergence in osteichthyes (bony vertebrates) estimated to have occurred around 450-million years ago (Buechi and Bridgham, 2017). The chondrichthyes include holocephalans (chimeras) and elasmobranchs (sharks and rays) which diverged around 300-million years ago (Irisarri et al., 2017). In the chimaera *Callorhinchus milii,* which was the first sequenced chondrichthyan genome (Venkatesh et al., 2014), all the genes encoding GPH subunits or subunits' ancestors (GPA2, CGA, GPB5, LHβ, FSHβ and two TSHβ, TSHβ1 and TSHβ2) and their receptors (FSHR, LHR and TSHR) were identified for the first time (Buechi and Bridgham, 2017; Maugars et al., 2014; Maugars and Dufour, 2015). Advances in the sequencing of elasmobranchian genomes (from 5 sharks and 4 rays, notably) are now making it possible to include elasmobranchs more widely in evolutionary analyses of GPHs/GTHs and their receptors, sequences of which have been identified in some sharks (e.g., *Scyliorhinus torazame* (Arimura et al., 2024; Hara et al., 2018)). In actinopterygians, tandem gene duplication of *lhr* led to duplicated *lhr1* and *lhr2*, conserved in teleosts (Maugars and Dufour, 2015). The teleost-specific whole genome duplication (3R) had no impact on the number of GTHR in teleosts, due to paralog gene losses early after 3R, leading to only one or two *lhr* and a single *fshr* (Chauvigné et al., 2010; Dufour et al., 2020; Maugars and Dufour, 2015). In primates, a particular feature has been the specific tandem gene duplication of *Lhb* at the origin of the chorionic gonadotropin subunit β (CGB) expressed in the placenta, giving the human chorionic gonadotropin (hCG) which has the ability to bind to LHR (Maston and Ruvolo, 2002). Interestingly, while the specificity of LHR and FSHR has long been established in mammals, and recently in the holocephalan *C. milii* (Buechi and Bridgham, 2017), FSHR appeared less discriminating in various teleosts and can be activated by LH in addition to FSH (Andersson et al., 2009; García-López et al., 2009; Kazeto et al., 2008; Suzuki et al., 2020). It has also been reported that LHR may also be activated by FSH in the rainbow trout, the zebrafish and the medaka (Burow et al., 2020; Sambroni et al., 2007; Xie et al., 2017) but not in the eel (Suzuki et al., 2020), suggesting that LH and FSH specificity might have varied during evolution.

The specificity of the GTHRs activation by GTHs is determined by their structures, which are mainly studied in humans. Alpha and β subunits are cystine-knot proteins containing disulfide bonds (SS) arranged in such a way that one SS bond crosses the ring formed by the other SS bridges (Lapthorn et al., 1994). Heterodimerization of the α and β subunits involves a low-affinity interaction between two regions named "seat", followed by wrapping of the α subunit by the "seat-belt" consisting of the C-terminus of the β subunit and finally locking of the specific SS bridge, called "buckle", involved in dynamic stability of the heterodimer (Belghazi et al., 2006; Burova et al., 2001; Galet et al., 2004; Hiro'oka et al., 2000; Jiang et al., 2014a; Lapthorn et al., 1994).

GTHRs are characterized by a large N-terminal ectodomain presenting a curved solenoid (horseshoe) with leucine-rich repeats domains (LRR), N-glycosylation sites and a "hinge" region containing a potentially sulfated tyrosine residue (reviewed in Helenius and Aebi, 2004; Vassart, 2004). Their transmembrane domain is characterized by seven transmembrane α-helix (7TM), three extracellular loops (EL) interacting with the "hinge" region (Jiang et al., 2014a) and three intracellular loops (IL) involved in the activation of G protein-dependent signaling pathways (reviewed in Johnson and Jonas, 2020; Nechamen et al., 2007). The C-terminal domain is characterized by various motifs involved in intracellular trafficking (reviewed in Dong et al., 2007), receptor desensitization, recycling and G_s-independent ERK1/2-mediated signaling in several mammals (Kara et al., 2006; Marion et al., 2006; Troispoux et al., 1999; Wehbi et al., 2010).

The study of the biological functions of gonadotropins and their receptors has been the subject of extensive research in vertebrates for many years. Classically, in osteichthyes, including actinopterygians such as teleosts and sarcopterygians (mammals, birds, amphibians), FSH and LH are secreted by pituitary gonadotroph cells into the general bloodstream to regulate gametogenesis and steroidogenesis in males and females (reviewed in Oduwole et al., 2021). Extra-pituitary expression of LH and FSH as well as of their receptors in extragonadal tissues have been also reported (Dufour et al., 2020; Johnson and Jonas, 2020). Surprisingly, few studies have been carried out on gonadotropins functions in the chondrichthyes, despite this group occupies an interesting phylogenetic position as the sister group to the osteichthyes. In chondrichthyes, *cga*, *fshβ* and *lhβ* were shown to be mainly expressed in the ventral lobe of the pituitary, and *fshr* and *lhr* expressed in the gonads as studied in the catshark *S. torazame* (Hara et al., 2018). However, these data are still insufficient to understand GTH functions in elasmobranchs, hence the present study during spermatogenesis in the small-spotted catshark *Scyliorhinus canicula*. In this species, spermatogenesis occurs in spermatocysts made up of synchronously-developing germ cells associated with Sertoli cells, forming a zonal arrangement of the spermatogenetic wave. Thus, on a cross section of the testis, zones corresponding to different stages of spermatogenesis are easily distinguishable and accessible (Bosseboeuf et al., 2014; Gautier et al., 2014; Loppion et al., 2008). A particular feature of the elasmobranch testis is the absence of differentiated Leydig cells, which, nevertheless, is a matter of debate. Indeed, previous studies showed rare undifferentiated "Leydig-like" cells in the testes of the sharks *Squalus acanthias* (Pudney and Callard, 1984) and *S. canicula* (Loir et al., 1995), but differentiated Leydig cells in the ray *Torpedo mormorata* (Prisco et al., 2002), which may correspond to the forerunners of true vertebrate Leydig cells of bony vertebrates (Callard, 1991; Engel and Callard, 2007). Another unique feature in elasmobranchs is the epigonal tissue, a lymphomyeloid tissue at the ventral testicular, where spermiation occurs (Manca et al., 2019). Anatomically, the male genital tract of elasmobranchs is complex. Spermatozoa converge through collecting tubules into efferent ducts, subsequently forming the epididymis, which also receives fluid from its adjacent Leydig's gland. The epididymis is followed by a deferent duct which is enlarged at its end and forms the seminal ampullae where spermatozoa are stored (Park et al., 2013).

In the present study, sequences of GTH subunits, including CGA, FSHβ and LHβ and of corresponding GTHRs have been identified in several elasmobranch species. Protein structures have been analyzed and expression patterns explored by real-time PCR and *in situ* approaches during spermatogenesis and in different tissues in the small spotted catshark as a model species. Functional hormone-receptor interactions have also been studied using recombinant proteins and *in vitro* bioassays. The results are discussed from an evolutionary perspective of the parallel evolution of endocrine signaling systems and gonadal structures.

2. Materials and Methods

2.1. Animals and tissue Sampling

In 2020, the catshark *Scyliorhinus canicula* was assessed as a least concern species in the red list of threatened species by the IUCN (International Union for Conservation of Nature). Sexually mature male (608 ± 137 g; 58 ± 3 cm) and adult female (647 ± 90 g; 57 ± 4 cm)

catsharks were fished during a CGFS (Channel Ground Fish Survey) campaign by IFREMER in the East Manche in September 2022 (Giraldo et al., 2022). Although females have an extended breeding season, with maximum egg-laying frequency from December to June (Sumpter and Dodd, 1979), females caught in September had their lowest gonadosomatic index and their ovaries consisted of post-ovulatory follicles and a few early vitellogenic follicles. Animals were maintained in natural seawater tanks at the marine station of the University of Caen Normandy (*Centre de Recherches en Environnement Côtier* (CREC), Luc-sur-Mer, France). The CREC experimental facilities were approved by the council department of population care under the A14384001 number (*Préfecture du Calvados*, France). Catsharks were allowed to acclimate at least 2 weeks before collection of the samples. Animals were killed by percussive blow to the head followed by sectioning and pithing of the spinal cord and exsanguination according to the European directive 2010/63/UE for care and use of animals. Testes, epigonal tissues, proximal and distal epididymis, seminal ampullae, myelencephalons, cerebellum, midbrains corresponding to diencephalon and mesencephalon and including pituitaries, forebrains, olfactory bulbs, eyes, thyroid glands, Leydig organs, spleens, livers, pancreas, duodenums, kidneys, rectal glands, gills, hearts and muscles were sampled from 14 males and myelencephalons, cerebellum, midbrains, forebrains, olfactory bulbs, ovaries, nidamental glands, oviducts, uterus and thyroid glands from 7 females and were transferred directly in liquid nitrogen before being stored at −80 °C until RNA extractions. Fresh testicular cross sections were transferred into ice-cold Gautron's buffer (pH 7.8, 890 mOsmol kg-1) (Gautron, 1978) completed by 58 mM trimethylamine-N-oxide (TMAO, Sigma, 317594), then microdissected into zones A, B, C and D corresponding to the zone of undifferentiated spermatogonia and cysts with spermatogonia, the zone of cysts with spermatocytes, the zone of cysts with early spermatids and the zone of cysts with late spermatids, respectively (Loir and Sourdaine, 1994). Tissues used for IHC and ISH were fixed in Gautron's buffer with paraformaldehyde 4 % before alcoholic dehydration and stocked in butan-1-ol at −20 °C.

2.2. Sequence searches

Protein sequences of CGA, FSHβ and LHβ subunits and their receptors were identified using BLAST searches, based on *C. milii* sequences (Buechi and Bridgham, 2017), against genomes of *Amblyraja radiata* (sAmbRad1.1.pri), *Carcharodon carcharias* (Marra et al., 2019), *Chiloscyllium plagiosum* (ASM401019v1), *Chiloscyllium punctatum* (Hara et al., 2018), *Pristis pectinata* (sPriPec2.1.pri), *Rhincodon typus* (Read et al., 2017), *S. canicula* (sScyCan1.2) and *S. torazame* (Hara et al., 2018) on NCBI (https://www.ncbi.nlm.nih.gov/genome/); of *Hemitrygon akajei* (sHemAka1.1) on Squalomix Blast Server (https://transcriptome.riken.jp/squalomix/blast/); and of *Leucoraja erinacea* (Wang et al., 2012) on Skatebase (http://skatebase.org). To assess the relationship between obtained sequences and their putative families, phylogenetic trees were built based on the previous work of Buechi and Bridgham, 2017 using the MAFFT (Multiple Alignment using Fast Fourier Transform) program, BMGE (Block Mapping and Gathering with Entropy) alignment curation and PhylML tree inference on NGPhylogeny online services (https://ngphylogeny.fr/workflows/oneclick/, Lemoine et al., 2019) with a bootstrap of 1000. Sequences used are listed (supplementary data, Excel). Obtained trees were finalized using iTOL online tool (https://itol.embl.de/, Letunic and Bork, 2021). Synteny analyses of *fshβ* and *lhβ* genes in *H. sapiens* and *S. canicula* were performed to verify the orthologs identified. The genes were mapped using NCBI's Genome Data Viewer (https://www.ncbi.nlm.nih.gov/genome/gdv/).

2.3. Structural analyses and 3D model building

Multiple alignments were performed using Clustal Omega package (https://www.ebi.ac.uk/Tools/msa/clustalo/, Sievers et al., 2011) with manual corrections to identified conserved structures (based on the knowledge in *H. sapiens* sequences). Signal peptides were predicted using predisi software (http://www.predisi.de/). Predictive models of GTHs/GTHRs interaction complexes of *S. canicula* α, β-subunits and the ectodomain of GTHRs were built using SWISS-MODEL (https://swissmodel.expasy.org/, Waterhouse et al., 2018), using the 4mqw.1 and 7fii.1 templates of *Homo sapiens*, and finalized using Swiss PDB Viewer program (Johansson et al., 2012). Obtained models were evaluated by retaining global sequence identities with the template, the highest GMQE score (Global Model Quality Estimate, Waterhouse et al., 2018), which depends on coverage, and the highest QMEANDisCo Global score (Studer et al., 2020), which evaluates the model "as is" without explicit coverage dependency. The same procedure was performed with *H. sapiens* sequences, as control, and for *C. milii* sequences. Using Swiss-PdbViewer (Johansson et al., 2012), predicted models were superimposed and the Root Mean Square Deviation (RMSD) were calculated and averaged by GTHs and by GTHRs.

2.4. Functional hormone-receptor interaction in in vitro assays

Synthetic pTarget plasmids containing *S. canicula* cDNA sequences for *fshr* (*sc-fshr*) or *lhr* (*sc-lhr*) were obtained from Twist Bioscience (San Francisco, USA) and synthetic pTarget plasmids containing fusion construct *gphβ-cga* were obtained from GenScript Biotech (Rijswijk, Netherlands). Human embryonic kidney (HEK293T) cells were transiently transfected with the synthetic plasmid using FuGENE HD (Promega) according to the manufacturer's instructions. Co-transfection was done with *gphr*/pTarget construct and a pTarget expression construct for the human $G\alpha_{16}$ subunit, a promiscuous G protein which can direct intracellular signaling of GPCRs to the release of calcium *via* the phospholipase Cβ pathway, regardless of the endogenous G protein coupling of the receptor. The pTarget ligand constructs were transfected in HEK293T cells at around 80 % confluence in 150 cm^2 flasks, then after 24 h of culture, the media were collected and concentrated using Amicon® 3 K filters (Millipore). Cells for negative control experiments were transfected with empty pTarget or *hs*Gα16 and empty pTarget. Activation of the *S. canicula* GTHRs by GTHs was monitored using a fluorescence-based calcium mobilization assay according to (Schwartz, 2021). Briefly, transfected HEK293T cells were loaded with Fluo-4 Direct (Invitrogen) for 1 day at 37 °C with 5 % CO_2. Excitation of the fluorophore was done at 488 nm. The calcium response was measured at 525 nm for 2 min using a Flexstation 3 (Molecular Devices) at 37 °C and analyzed using SoftMax Pro (Molecular Devices). For analysis of the activation of the Gαs/adenylyl cyclase/cAMP/PKA pathway, transfected cells were incubated with Glosensor cAMP reagent (4 % final concentration in media) (Promega) for 2 h at room temperature prior the injection of the ligands (*sc*FSHβ-*sc*CGA, *sc*LHβ-*sc*CGA or *sc*TSHβ-*sc*CGA, as negative control and intracellular cAMP concentration was estimated by the luminescence response measured at 37 °C for 30 min using the Flexstation 3.

To determine the absolute concentration of the ligand produced, an initial proteomic analysis of the ligand-containing media was carried out using high-resolution nanoLC-ESI-MS/MS to identify a peptide resulting from trypsin digestion of the common α-subunit (CGA). The criteria for the choice of this peptide were the absence of cysteine residue, the absence of post-translational modifications, and a number of amino acids superior to 5. The selected peptide (VTLMGNLK) was synthesized by CliniSciences (Nanterre, France) and used as an internal quantity marker. The standard curve was established, ranging from 16.3 pg/µl to 666 pg/µl, and the equation obtained was $y = 400{,}05x - 6339{,}1$ ($R^2 = 0{,}9967$) where "y" was the peak area of the peptide and "x" the concentration. Half maximum effective concentrations (EC_{50} values) and activation percentages were calculated with 95 % confidence intervals (profile likelihood) from sigmoidal dose–response equations which were constructed with a nonlinear regression analysis using Prism 5.0 (GraphPad Software, USA). A more sensitive *in vitro* bioassay has also been used, according to Klett and Combarnous, 2021. Developed to

measure luteinizing hormone and chorionic gonadotropin concentrations in the plasma of most mammalian species, this system used mLTC Leydig cell line (ATCC CRL-2065) transiently co-transfected with the cAMP Glosensor reporter gene (Promega) and the *gthr* of interest. The scGTHb-scCGA ligands were produced in CHO-K1 cell line (ATCC CCL-61), and the supernatants were tested on mLTC cells previously pre-incubated for 2 h in the presence of 10^{-3}M IBMX (3-isobutyl-1-methyl-xanthine), 10^{-5}M forskolin, 10^{-8}M oxytocin (OXT) and 1 % Glosensor cAMP reagent. Intracellular cAMP concentration was estimated by the luminescence response measured at 28 °C for 60 min using a Polarstar Optima (BMG Labtech Sarl, Champigny sur Marne, France).

2.5. Reverse transcription and real-time PCR

Total RNAs were extracted from *S. canicula* tissues using Tri-Reagent (Sigma-Aldrich, 93289) before purification with the NucleoSpin RNAII columns kit (Machery-Nagel). They were quantified on a NanoDrop™ 2000 (Thermo Scientific) and their qualities were analyzed on an Agilent 2100 Bioanalyzer (Agilent). Obtained RINs (RNA integrity number) were greater than 7. For tissue distribution, real-time PCR was performed independently for three animals (N=3) in triplicate (n = 3) except for testes (zone A, B, C and D) and epigonal tissues where six animals were used (N=6, n = 18). The CFX Connect Detection System (Bio-Rad) was used for real-time PCR analyses. Two hundred and seventy ng of total RNAs were treated with 1U of RQ1 DNase (Promega, M6101) (37 °C/20 min) following by the reverse transcription using 1 ng of random hexanucleotide primers (Promega, C1181), 0.5 mM dNTPs and 200 U of M−MLV Reverse Transcriptase (Promega, M1701) then the reactions were stopped (70 °C/5min). The gene-specific primers were designed using Primer-BLAST (https://www.ncbi.nlm.nih.gov/tools/primer-blast/, Ye et al., 2012) with manual corrections to take into account the following criteria: length between 18–22 bp, GC content over 50 %, Tm close to 60 °C and generation of an 150–200 bp amplicon (supplementary data Table S1). The real-time PCR monitoring of amplifications (5 ng of cDNA, 40 cycles: 95 °C/15 s, 60 °C/45 s), the GoTaq®qPCR Master Mix (Promega, A6001) was used and melt curve analysis and efficiency tests were carried out to ensure the primers amplified a single product with 90–110 % efficiency. The Ct values were read at 200 relative fluorescence units and normalized against the 5S RNA (Redon et al., 2010), using the ΔC_t method (Schefe et al., 2006). The $2^{-\Delta\Delta Ct}$ method (Livak and Schmittgen, 2001) allowed to calculate the expression variations based on the mean ΔC_t of all tissues. Comparison of the Ct 5SRNA/total RNA ratio between tissues shown no significant difference using none parametric Kruskal-Wallis test with a P-value of 0.11 (supplementary data Fig. S1). Statistical analyses were performed using the non-parametric Mann-Whitney U (based on the previous Shapiro-wilk test results) test for P-value < 0.05.

2.6. In situ hybridization (ISH)

Digoxigenin-conjugated riboprobes were synthesized from cDNA clones produced with specific primers (supplementary data Table S1). The resulting amplicons were cloned in pCR™II-TOPO™ Vector by TA cloning and then transformed in chemically competent *E. coli* using the TOPO TA Cloning kit (Invitrogen, k461020). After cultures, plasmids were purified using the Wizard® Plus SV Minipreps (Promega, A1340) then the digoxigenin-conjugated riboprobes were generated using M13 PCR on 100 ng of plasmids with 1 mM $MgCl_2$, 0.2 mM of each dNTPs, 0.4 μM M13 primer and 0.625 U GoTaq® Flexi DNA Polymerase (Promega, M8291). The cycling parameters were as follows: 1X(95 °C, 5 min), 30X[(95 °C, 30 s), (60 °C, 45 s), (72 °C, 1min30s)], 1X(72 °C, 5 min). PCR products were quantified using Nanodrop 2000 spectrophotometer (Thermo Scientific) and then purified using the NucleoSpin RNA Clean-up (Marcherey-Nagel, 740948.50). The size checking was done using gel migration. *In vitro* transcriptions were carried out for 3 h at 37 °C on 1.2 μg PCR products with 25 U RNAsin, 25 U T7 or SP6 polymerase, 10 mM dithiothreitol, 1 mM rATP, rCTP and rGTP, 0.65 rUTP, and 0.35 digoxigenin-UTP (Roche, 03359247910) using the Riboprobe® Combination Systems (Promega, P1460). DNAs were digested with 2 U RQ1 DNAse (Promega, M6101) for 30 min at 37 °C. The resulting riboprobes were purified and their qualities were checked by dot blots on PVDF membrane. Paraffin slices (5 μm) were incubated at 61 °C to facilitate deparaffinization using Roti-histol (sigma, 6640.6). Hydration was achieved by successive ethanol baths (100 %, 95 % and 70 %), then by PBS. Between each of the following treatments, slices were washed into PBS. Slices were treated with 4 % PFA in PBS, with 5 μg/ml proteinase k in Tris buffer for 4 min, with 4 % PFA in PBS, with 100 mM Triethanolamine in 25 % acetic acid, then with 100 mM glycine in tris buffer. Tissues were incubated for 1 h at 65 °C with the hybridization mix (50 % deionized formamide, 1X saline-sodium citrate (SSC), 0.5 M Ethylenediaminetetraacetic acid (EDTA), 10 % Tween 20, 1X Denhardt'solution, 28 mg/ml Dextran sulphate, 0.1 mg/ml heparin, 10 % Chaps, 0.5 mg/ml tRNA). Then, 0.1–0.5 ng/μl riboprobes in hybridization mix were incubated overnight at 65 °C. Slices were washed using successive baths of SSC (1X and 1.5X at 65 °C, 2X at 37 °C, 2X with 0.2 μg/ml of RNAse A (Promega, A797C) at 37 °C, 2X, and 0.2X at 60 °C) before maleic acid buffer baths with 0.3 % triton (MABT). For immunostaining and revelation, the DIG Nucleic Acid Detection kit (Roche, 11175041910) was used. Tissues were incubated 3 h in blocking solution then, overnight at 4 °C, with 100 μl per slice of 1/2000 v/v anti-digoxigenin-AP-conjugate antibody 750 U/ml. According to the kit guidelines, slices were washed in MABT baths before being developed overnight at 4 °C in NBT/BCIP. Finally, slices were mounted in Mowiol mounting medium and then dried for 48 h at 4 °C, before being observed using a Nikon eclipse 80i microscope.

2.7. Immunohistochemistry (IHC)

Tissues embedded in paraffin were cut into 5 μm sections with a microtome (Leica, Histocore Autocut R). The slices were deparaffined in roti-histol baths (Roth, 6640.2), rehydrated using successive ethanol dilutions (100 %, 96 %, 75 % and 50 %) and washed in PBS before antigen unmasking (2x 90 s, micro-waves 600 W followed by a 1 h cooling period). Endogenous peroxidase activities were blocked with 3 % hydrogen peroxide in PBS, and non-specific labeling was blocked using PBS with 0.1 % Triton and 1 % BSA. Diluted primary antibodies in Antibody Diluent (Abcam, ab64211) were incubated overnight at 4 °C then washed in PBS before a 2 h incubation with the corresponding secondary antibodies at room temperature. After washing, the DAB Substrate Kit (3.3′-Diaminobenzidine, Abcam, ab64238) was applied until staining (2–60 min). Then, the slices were counterstained with Groat's haematoxylin and rinsed with running water. They were dehydrated into successive ethanol baths (50 %, 75 %, 96 % and 100 %), then into roti-histol (Roth, 6640.2) before to be mounted into roti®histokit media (Roth, 6638.1). Images were taken using an optical microscope (Nikon, eclipse 80i) equipped with NIS-Elements D 3.0 software (Nikon Instruments). The primary antibody targeting PCNA (proliferating cell nuclear antigen, Mouse monoclonal PCNA (rat) antibody, 1:500, Invitrogen, 13–3900 PC-10) was used as quality control for testes tissues and the same results as Loppion et al., 2008 were obtained (not shown). Primary antibodies were used at the indicated dilution: mouse monoclonal anti-human FSHR antibody (1:500, Abcam, ab219312), rabbit polyclonal anti-human FSHR antibody (1:500, Abcam, ab137695), mouse monoclonal anti-human LHR antibody (1:100, Abcam, ab218447). Secondary antibodies were used at the indicated dilution: Goat Anti-Mouse IgG H&L, horseradish peroxidase (HRP) polymer (1:1, Abcam, ab214879) and Goat Anti-Rabbit IgG H&L, HRP polymer (1:1, Abcam, ab214880).

2.8. Immunocytofluorescence (ICF)

Immunocytofluorescence detections were performed to verify the

expression of recombinant proteins and the antibodies' specificity used in IHC analyses. HEKT293T cells transfected with pTarget-*scfshr* or pTarget-*sclhr* plasmids were washed twice using PBS with 1 % BSA, collected and fixed with 4 % PFA for 15 min before attachment to polysine slides (Epredia). The cells were permeabilized with 0.1 % Triton in PBS buffer with 1 % BSA for 5 min then incubated with primary antibodies, overnight, at 4 °C. The cells were then washed and incubated for 2 h with secondary antibodies, at room temperature. After washes, the cells were mounted in Prolong™ Gold Antifade Mountant with 40,6-diamidino-2-phenylindole (DAPI) (P36935). Images were taken using an optical microscope (Nikon, eclipse 80i) equipped with NIS-Elements D 3.0 software (Nikon Instruments) with the same exposure time for each antibody, independently of the sample tested. The same primary antibodies as in IHC experiments were used: mouse monoclonal anti-human FSHR antibody (1:100, Abcam, ab219312), rabbit polyclonal anti-human FSHR antibody (1:100, Abcam, ab137695) and mouse monoclonal anti-human LHR antibody (1:100, Abcam, ab218447). Secondary antibodies were used at the indicated dilution: Goat anti-Rabbit IgG (H+L), Alexa Fluor™ 488 (1:250, Invitrogen, A-11008) and Goat anti-Mouse IgI (H+L), Alexa Fluor™ 488 (1:250, Invitrogen, A-11001).

3. Results

3.1. Genome searches of GTHs and GTHRs in elasmobranchs

Sequence searches were carried out on the basis of sequences identified in *C. milii* and some predicted sequences available in the NCBI database for *S. canicula*. A first analysis using the *C. milii* FSHR sequence blasted the LHR isoform XP_038666531.1 of *S. canicula* (loci LOC119973089), whereas the LHR sequence of *C. milii* blasted another LHR-like sequence of *S. canicula* (XP_038650550.1, loci LOC119964708). Further analyses of the *S. canicula* genome (sScyCan1.2) with sequences from a transcriptome library (S. Mazan, personal communication) enabled us to identify the FSHR and LHR sequences of *S. canicula* and the incorrect annotation of the LHR isoform XP_038666531.1, which in fact corresponded to FSHR. Then, the subsequent phylogenetic analysis, including sequences of 159 GTH subunits and 91 GTHRs, validated their annotations. Molecular phylogeny of the CGA subunits (supplementary data Fig. S2) showed that the chondrichthyan sequences are grouped in accordance of species phylogeny and that the holocephalan CGA rooted with the elasmobranchian sequences (batoidea and selachii groups). In addition, chondrichthyan CGA sequences are grouped with those of the sarcopterygii and segregated from those of the actinopterygii. Molecular phylogeny of the β subunits sequences (supplementary data Fig. S3) showed that the chondrichthyan FSHβs sequences segregated between the actinopterygian and sarcopterygian FSHβs sequences. The holocephalan FSHβ sequence was found between the batoidea and Selachii sequences. Contrary to what was obtained for chondrichthyan FSHβ sequences, the chondrichthyan LHβ sequences rooted with the actinopterygian and sarcopterygian sequences. As observed for FSHβ sequences, the holocephalan LHβ sequence was found between the batoidea and Selachii sequences. In the GTHRs phylogenetic tree (supplementary data Fig. S4), both chondrichthyan FSHRs and LHRs sequences are grouped with those of the sarcopterygii and segregated from those of the actinopterygii. The holocephalan GTHR sequences rooted with the corresponding elasmobranch (batoidea and selachii) sequences.

3.2. Predicted structural domains of GTHs and GTHRs

The primary structures of elasmobranchs GTHs and GTHRs were analyzed in relation to knowledge of human orthologs. Alignment of the chondrichthyan CGA sequences has shown 10 conserved cysteines (C), 2 putative N-glycosylation sites and a 'seat' region conserved in all elasmobranchs with a lysine (K) residue instead of a valine (V) in the holocephalan sequence (supplementary data Fig. S5). The alignment of the chondrichthyan β-subunit sequences, evidences 12 conserved C residues, including the three characteristic cysteines of the "seat-belt" (C10, C11, C12), and 1 (LHβ) or 2 (FSHβ) N-glycosylation sites (supplementary data Fig. S6). The "seat" region (amino acids 55 to 59) is conserved in selachii FSHβs with an alanine (A) instead of a serine (S) in the holocephalan and batoidea sequences. In the 'seat' region of elasmobranchs LHβs, the threonine (T) of the holocephalan was substituted by a serine (S), except in *S. canicula* where it was substituted by a glycine (G).

Multiple alignments of the protein sequences of FSHR (supplementary data Fig. S7) and LHR (supplementary data Fig. S8) have shown, in their large extracellular domains, 35 well-conserved leucine (L) residues, 3 (FSHR) or 5 (LHR) putative N-glycosylation sites, 10 (FSHR) or 2 (LHR) conserved cysteines (C) and the perfectly conserved putatively sulfated tyrosine in the FSHR and LHR sequences. The putative limit between the solenoid and the "hinge" region was predicted. The transmembrane region of the chondrichthyan GTHRs was composed of 7 putative α-helical transmembrane domains (TM), 2 conserved cysteines, one APPL1, one ERW, one Ubiquitin interaction and PKC2 binding domain, and one BXXBB putative motif. A putative L-palmitoyl site was identified in the TM helix 7 of FSHRs. The C-terminal region of GTHRs exhibits a putative $F(X)_6LL$ motif, a S/T cluster, a second BXXBB and a second L-palmitoyl site. *S. canicula* FSHβ and LHβ annotations were validated by synteny (Fig. 1A). Amino acid residues involved in the FSHβ or LHβ binding specificity to their receptors were analyzed and appeared conserved between *S. canicula* FSHβ, *S. canicula* LHβ and *H. sapiens* FSHβ sequences (Fig. 1B).

3.3. Predicted models of the GTHs/GTHRs interacting complexes

The FSH/FSHR interacting models, obtained with SWISS-MODEL and using the 4mqw.1 and 7fii.1 templates of *H. sapiens*, showed overall sequence identities relative to the 4mqw.1 template of 56.20 % and 51.55 % for *C. milii* and *S. canicula*, respectively (Table 1). However, compared with the human model, the GMQE scores were 0.08 lower for both, and the QMEANDisCo Global scores were 0.08 and 0.09 lower for the *C. milii* and *S. canicula* models, respectively, reinforcing the models obtained. Better scores were obtained for the LH/LHR interacting models with 66.42 % and 67.07 % global sequence identities compared to the *H. sapiens* 7fii.1 template, a GMQE score 0.03 and 0.09 lower, and a QMEANDisCo Global score 0.05 and 0.10 lower compared to the human model, for the *C. milii* and *S. canicula* models, respectively (Table 1). The predicted FSH/FSHR model obtained for *S. canicula* showed that the main characteristic 3D structures involved in αβ subunits interactions were conserved with the cystine-knot (Fig. 1C1), the "seat" (Fig. 1D1) and the "seatbelt" (Fig. 1D2) structures. The solenoid and the "hinge" regions of the FSHR ectodomain were also represented (Fig. 1D). The CGA/GTHβ dimers showed the interaction between the two "seat" regions (Fig. 1D1), the "seatbelt" girdling the CGA subunit and the "buckle" in place (Fig. 1D2). FSH was positioned between the concave surface of the solenoid and the "hinge" of the receptor (Fig. 1D4) with the putative sulfotyrosine residue of the "hinge" towards the hormone binding pocket (Fig. 1D3). Similar results were obtained for LH/LHR interaction (data not shown). Superimpositions of the 3D structures between the three species were realized for the two receptors and the two hormones in order to analyze the most variable protein structure. The results showed that the GTHR models had very low and similar Root Mean Square Deviations (rmsd), ranging from 0.67 to 0.82 Å, for the solenoids, but very high rmsd for the "hinge" regions, ranging from 34.04 to 57.39 Å (Fig. 1E,F). The superimpositions of the GTHs models have shown highly similar rmsd, ranging from 0.17 to 0.22 Å (Fig. 1G,H).

3.4. Functional hormone-receptor interactions in vitro assays

HEK293T cells co-expressing *sc*FSHR/*hs*Gα_{16} subunit or *sc*LHR/*hs*Gα_{16} were stimulated by serial dilutions of conditioned medium from

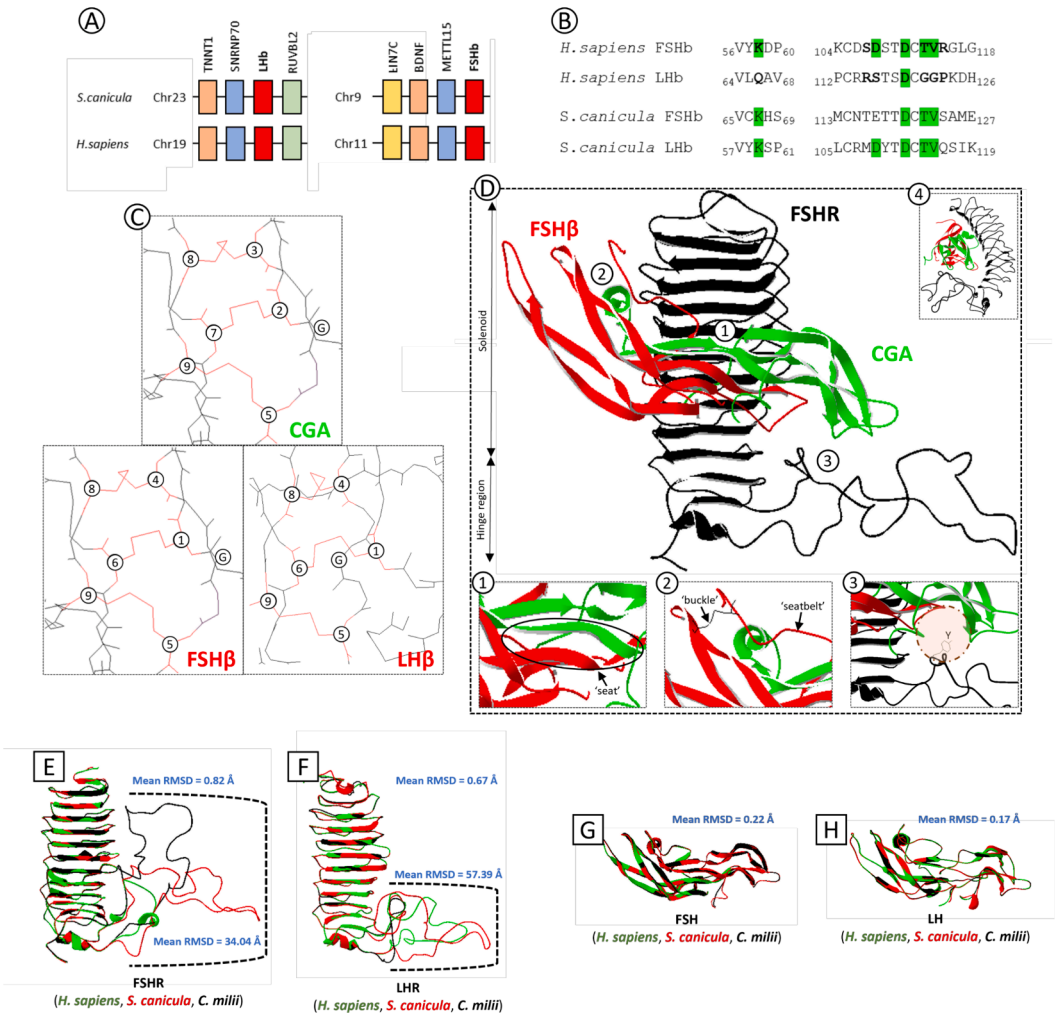

Fig. 1. Synteny and *in silico* analysis of the 3D structures of the GTHs/GTHRs interaction complexes, in *S. canicula*, based on the *H. sapiens* templates. (A) Synteny of the genomic region flanking *fshβ* and *lhβ* genes in *H. sapiens* and *S. canicula*. The chromosome numbers are indicated. The *H. sapiens* genomic regions were used as templates. (B) Multiple alignments of FSHβ and LHβ receptor-binding sites. Residues known to be involved in ligand-receptor interaction are shown in bold. Corresponding conserved residues are highlighted in green. (C) Predictive models of the 8-aa-ring cystine-knot structure for *S. canicula* CGA, FSHβ and LHβ. The conserved cysteines and the glycine are underlined by circled numbers and G, respectively. (D) The model of the 3D FSHβ-CGA/FSHR interaction complex in *S. canicula*. FSHβ is colored in red, CGA in green and the FSHR N-terminal ectodomain (solenoid and hinge) in black. The inserts correspond to part of the global view identified by numbers: (1) the interaction between the FSHβ and CGA 'seat' interface regions, (2) the 'seatbelt' region which wrap the CGA and forming the 'buckle' disulfide bond (SS), (3) the putative sulfotyrosine residue found in the FSHR hinge which is oriented toward the FSH pocket (brown area) and (4) the lateral view of the interacting complex with the FSH positioned between the concave surface of the solenoid and the hinge. 3D interacting models were constructed from the *H. sapiens* 4mqw.1 template for FSHβ-CGA/FSHR and from the 7fii.1 for LHβ-CGA/LHR (data not shown). (E-F) Superimpositions of the predicted models of the *S. canicula*, *C. milii* and *H. sapiens* FSHRs and LHRs. G-H. Superimpositions of the predicted models of the *S. canicula*, *C. milii* and *H. sapiens* FSHs and LHs. The mean of Root Mean Square Deviations (RMSD), in ångström (Å), were calculated to illustrate the global superimposition correspondences. The dotted brackets highlight the hinge regions.

Table 1
Efficiency (EC_{50}) and efficacy (Emax) of *sc*FSHβ-*sc*CGA (*sc*FSH) and *sc*LHβ-*sc*CGA (*sc*LH) on *sc*FSHR and *sc*LHR.

	Efficiency (EC_{50}) nM		Efficacy (Emax) %	
	*sc*FSH	*sc*LH	*sc*FSH	*sc*LH
*sc*FSHR	0.383 ± 0.019	0.103 ± 0.005	100.00 ± 3.58	78.18 ± 4.15
*sc*LHR	N/A	0.279 ± 0.014	N/A	100.00 ± 2.56

N/A: not applicable.

cells expressing the monocatenary recombinant protein *sc*FSHβ-*sc*CGA, *sc*LHβ-*sc*CGA or, as control, *sc*TSHβ-*sc*CGA (Fig. 2) (Table1). Dose-response analyses based on Ca^{2+} detection have shown that *sc*FSHβ-*sc*CGA and *sc*LHβ-*sc*CGA were able to activate *sc*FSHR-expressing cells with a higher EC_{50} with *sc*FSH (0.383 ± 0.019 nM) than with *sc*LH (0.103 ± 0.005 nM) (Fig. 2A; Table1). However, the maximum response for *sc*FSHR was higher with *sc*FSHβ-*sc*CGA (100.00 ± 3.58 %) than with *sc*LHβ-*sc*CGA (78.18 ± 4.15 %). The recombinant *sc*TSHβ-*sc*CGA protein was unable to activate *sc*FSHR. Cells expressing *sc*LHR were activated by the recombinant *sc*LHβ-*sc*CGA protein, with an EC_{50} of 0.279 ± 0.014 nM, but not with *sc*FSHβ-*sc*CGA or *sc*TSHβ-*sc*CGA (Fig. 2B; Table1). Analyses of cAMP production in response to recombinant proteins in HEK293T cells expressing *sc*FSHR or *sc*LHR, without co-transfection with the human *hs*$G\alpha_{16}$ subunit, didn't allow to detect any significant responses. However, using the highly sensitive *in vitro* bioassay in mLTC Leydig cell line, dose–response was obtained for *sc*FSHβ-*sc*CGA after transfection with *scfshr*. In this system, *sc*FSHβ-*sc*CGA and also *sc*LHβ-*sc*CGA in a lesser extent but not *sc*TSHβ-*sc*CGA activated cAMP accumulation through *sc*FSHR (supplementary data Fig. S9).

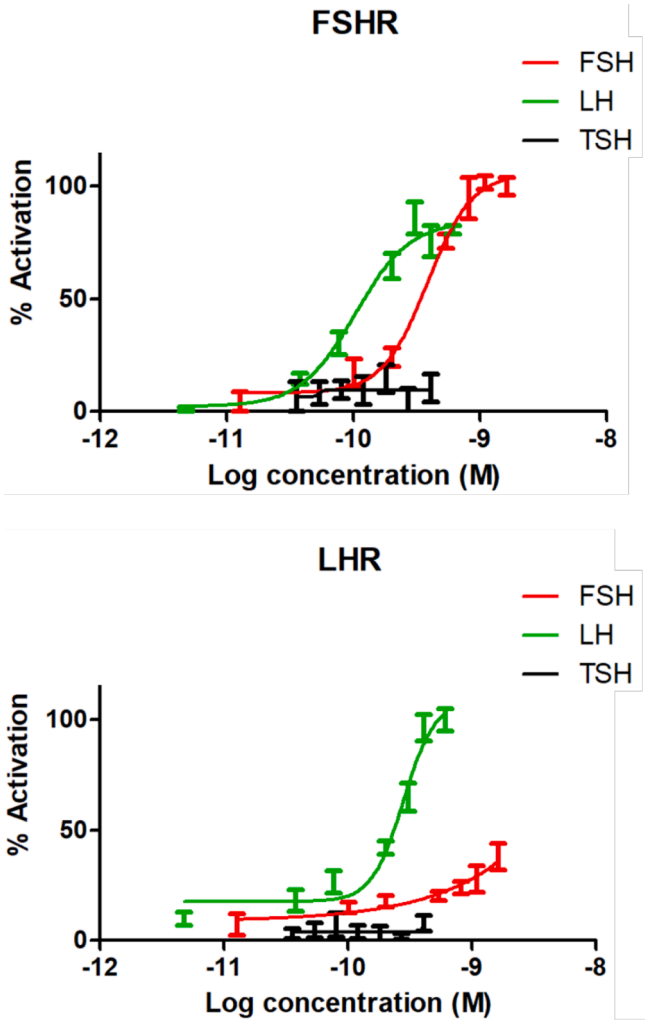

Fig. 2. Dose-responses of HEK293T cells co-expressing *sc*GPHR/*hs*Gα_{16} induced by recombinant *sc*FSHβ-*sc*CGA (*sc*FSH) or *sc*LHβ-*sc*CGA (*sc*LH). (A-B) Dose-dependent calcium responses of HEK293T cells co-expressing *sc*GPHR/*hs*Gα_{16} treated with serial dilutions of conditionned medium from HEK293T transfected with corresponding pTarget *ghpβ-cga* plasmids. All experiments were performed in duplicate and the most representative was selected for ligand absolute quantification using high-resolution nanoLC-ESI-MS/MS. Data are shown as relative (%) to the highest value (100 % activation) for a given ligand and represent the mean of an experiment (n = 3).

3.5. Relative expression profiles of cga, fshβ and lhβ transcripts in s. Canicula tissues

The expression profiles of transcripts of the genes coding for gonadotropins subunits were explored by real-time RT-PCR in 12 tissues including the male genital tract (testis, epididymis with Leydig's gland, seminal ampulla), ovary, and different parts of male and female brains. As expected, the highest expression of all transcripts was observed in the midbrain (including the pituitary gland) of males and females with a three-fold lower relative value for *cga* mRNAs in the male midbrain (2.6 ± 0.9) than in the female midbrain (7.7 ± 0.4) (Fig. 3). Expression of *cga* was also observed in others parts of the brain in both males and females, in the testis and at low levels in epididymis and ovary (Fig. 3A). Both *fshβ* and *lhβ* were highly expressed in the midbrain/pituitary in both sexes, about fifteen times less in other parts of the brain and not detectable in the male tract and ovary (Fig. 3B,C).

3.6. Relative expression profiles of fshr and lhr transcripts in s. Canicula tissues with a focus in the male genital tract

The expression profiles of *fshr* and *lhr* transcripts in 35 different tissues showed that *fshr* expression was mainly observed in testicular zones and in ovary and at very low levels in epigonal tissue and in male and female parts of the brain (Fig. 4A). According to the spermatogenic wave, *fshr* was significantly higher expressed in the testicular zone A containing the germinative area and cysts with spermatogonia and was two-fold less expressed in the following stages of spermatogenesis (zones B, C and D) (Fig. 4B). Very low expressions were observed in epididymis and seminal ampullae. Levels of *fshr* transcripts in the ovary were of the same order of magnitude as in testicular zone A. With regard to *lhr*, a broader tissue-expression profile was observed with higher transcript levels in the testicular zone A, but at lower levels than *fshr*, the distal epididymis associated with leydig's gland, the seminal ampullae containing spermatozoa, the lymphomyeloid Leydig organ, the thyroid and kidney in males (Fig. 4A,C). In females, *lhr* was weakly expressed in the ovary but highly expressed in the nidamental gland and oviduct, as well as in the myelencephalon (Fig. 4A,C).

3.7. Immunohistochemistry (IHC) and in situ hybridization (ISH) on s. Canicula tissues, with a focus on the male genital tract

In situ analyses were carried out in genital tract tissues, based on levels observed by real-time PCR, to identify the cell types expressing the receptors. In order to support the antibodies used, immunocytofluorescence was performed on HEK293T cells expressing *sc*FSHR or *sc*LHR (Fig. 5). The results showed that both the mouse monoclonal anti-human FSHR antibody and the rabbit polyclonal anti-human FSHR antibody exhibited a specific signal in the cytoplasm (probably in endoplasmic reticulum) and cell membrane of *sc*FSHR-expressing cells compared with the control corresponding to cells transfected with the empty plasmid. Similarly, the mouse monoclonal anti-human LHR antibody showed a specific signal in cytoplasm (probably in endoplasmic reticulum) and cell membrane of *sc*LHR-expressing cells compared with the control.

In function of the spermatogenetic waves, immunohistochemistry targeting FSHR (using the rabbit polyclonal anti-human FSHR antibody) showed a staining of individual spermatogonia (Fig. 6A1), corresponding to potential spermatogonial stem cells, and of spermatogonial progenitors (Fig. 6B1) in the germinative zone of the testis. Subsequently, spermatogonial staining, corresponding to differentiated spermatogonia, was still observed in the cysts formed, but basal and adluminal cystic staining also appeared, suggesting FSHR expression in Sertoli cells (Fig. 6C1). FSHR was further expressed in spermatocytes (Fig. 6D1), round spermatids (Fig. 6E1) and their associated Sertoli cells. The staining observed in the cytoplasmic compartment surrounding the Sertoli cell nucleus in the basal position of the cyst at the round (Fig. 6E1) and elongated (Fig. 6F1) spermatid stages, allowed us to ensure the localization of FSHR in Sertoli cell. Furthermore, this stage- and cell-dependent FSHR expression pattern was consistent with ISH results which have shown the localization of *fshr* transcripts in early spermatogonia (Fig. 6A2) and, subsequently, when the cyst was formed (Fig. 6B2), in both Sertoli cells and germ cells (Fig. 6C2-E2) with the exception of late stages where only Sertoli cells remained stained, elongated spermatid bundles being unstained (Fig. 6F2). Analyses using mouse monoclonal anti-human FSHR antibody revealed very similar expression patterns (supplementary data Fig. S10).

Expression analyses of LHR by IHC showed similar localizations to those of FSHR. LHR staining was observed into undifferentiated spermatogonia and somatic precursors (Fig. 6A3-B3). Then, when cysts were formed, in Sertoli cells with adluminal (Fig. 6C3) and basal staining (Fig. 6C3-F3), and in germ cells (Fig. 6C3-F3). However, in cysts with bundles of elongated spermatids (Fig. 6F3) and at this level of observation, it remains difficult to determine whether the expression is

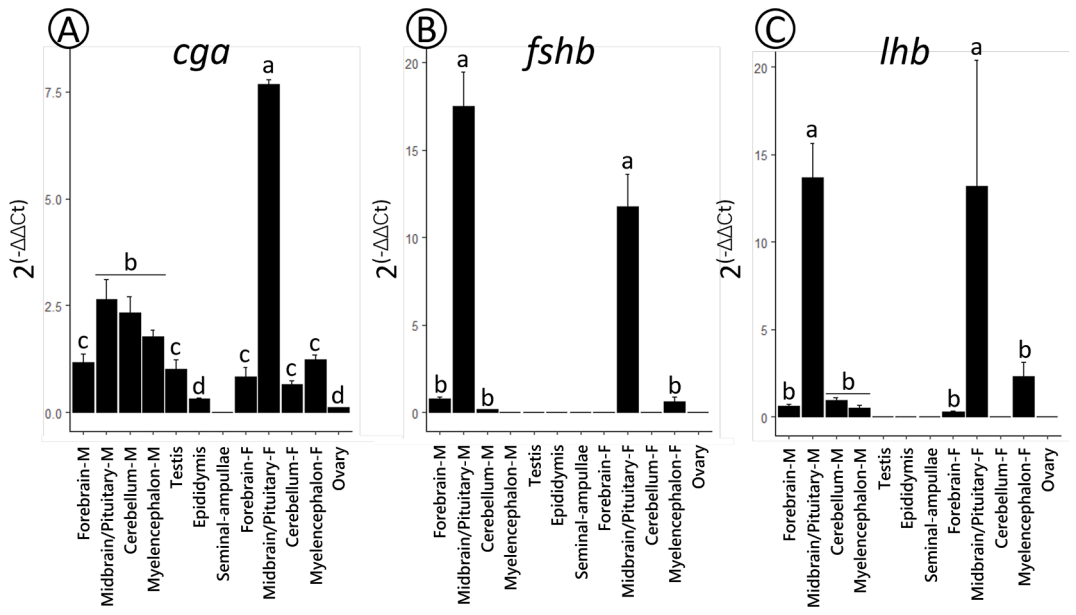

Fig. 3. Relative expression profiles of *cga*, *fshβ* and *lhβ* transcripts in different tissues of *S. canicula*. Messenger RNA levels were assayed for *cga* (A), *fshβ* (B) and *lhβ* (C) by real-time PCR in various tissues of adult catshark: forebrain, midbrain/pituitary, cerebellum, myelencephalon, testis, epididymis, seminal ampullae, ovary. Each tissue was analyzed in triplicates from three animals (N=3; n = 9). M, Male; F, Female.

located in sertolian projections between spermatids heads or in germ cells. In accordance with IHC results, ISH showed *lhr* transcripts in undifferentiated spermatogonia and their adjacent undifferentiated somatic cells (Fig. 6A4-B4). Expression of *lhr* was still observed in Sertoli cells and germ cells at the stages of differentiated spermatogonia (Fig. 6C4), spermatocytes (Fig. 6D4), round spermatids (Fig. 6E4), and elongated spermatid bundles (Fig. 6F4).

To partially conclude on these *in situ* results and taking into account the difficulty to certify more precisely the localization of expressions, it appeared that both *fshr* and *lhr* were expressed at all stages of spermatogenesis, reflecting a potential redundancy of functions associated with these receptors. For this reason, *in situ* expression analyses were extended to ovarian follicles containing differentiated granulosa and theca cells, used as a control rather than for in-depth study. In these follicles, FSHR protein and *fshr* mRNA were only expressed in granulosa cells (Fig. 7A4-A5), whereas LHR protein and *lhr* mRNA were only expressed in theca cells (Fig. 7A2-A3).

In situ analyses were completed with studies on the epigonal tissue, the testicular tubules (stem, branched and collecting tubules), the epididymis and its associated Leydig's gland. Surprisingly, strong staining was observed in the epigonal tissue for both *fshr*/FSHR and *lhr*/LHR, apparently associated with granulocytes and myelocytes but not lymphocytes and erythrocytes (Fig. 6G1-G4). In the following part of the male internal genital tract, the expressions of both *lhr*/LHR and *fshr*/FSHR were observed in epithelial cells of the stem and branched tubules (Fig. 7B2-B5), collecting tubules (Fig. 7C2-C5) and of *lhr*/LHR in the epithelial cells of the proximal (Fig. 7D2-D3) and distal epididymis (Fig. 7E2-E3) and Leydig's gland (Fig. 7F2-F3).

4. Discussion

4.1. Structures and interactions of gonadotropins with their receptors

One of the aims of our study was to complete the characterization of gonadotropins and their receptors in elasmobranchs on the basis of a previous work that identified FSH, LH and receptors in *C. milii* (Buechi and Bridgham, 2017). The primary structures of the orthologs identified in elasmobranchs show that the CGA, FSHβ and LHβ subunits display the characteristic "seat" and "seat-belt" regions, the conserved cysteines, including the ones forming the 8-aa-ring cystine-knot, and the putative N-glycosylation sites. As highlighted in the human models, experimentally validated (Duan et al., 2021; Jiang et al., 2014a, 2014b), these conserved tertiary structures are essential for ligand-receptor interaction with the involvement of the "buckle", the "seat-belt" and the potential interaction between the two "seat" regions of CGA and GTHβ. These results underline the high conservation of GTH structures from their emergence in chondrichthyes to mammals. Compared with the GTHRs of holocephalan *C. milii* (Buechi and Bridgham, 2017) and *H. sapiens* (Ulloa-Aguirre et al., 2018), the primary structures of the FSHR and LHR identified in elasmobranchs are highly conserved with the leucine-rich solenoid, hinge, N-glycosylation and sulfation sites and display the receptor family typical features in their ectodomain. On the basis of 3D models, while a high similarity in tertiary solenoid structures is observed between GTH receptors from *H. sapiens*, *C. milii* and *S. canicula*, a significant difference is observed between receptor hinges from the three species, both in size and conformation except for the potentially sulfated tyrosine which contributes greatly to hormone recognition and receptor activation (Jiang et al., 2014a,b). Interestingly, a very recent work on the functional characterization of FSHR and LHR in the cloudy catshark *S. torazame* has shown that a LHR variant without exon 10, encoding part of the hinge and also corresponding to the *C. milii* and *S. canicula* LHRs used in our 3D modeling, exhibited basal cAMP activity (Arimura et al., 2024), reinforcing the role of the hinge in the receptor activation.

For both receptors, FSHR and LHR, the primary structure of the seven transmembrane α-helixes is also conserved with APPL1, ERW, BXXBB, ubiquitin interacting and PKC2 binding domains in intracellular loops 1, 2 and 3, respectively. The second BXXBB, $F(X)_6LL$, L-palmitoylation and S/T motifs are also conserved in the intracellular Ct domain. Taken together, this suggests the ability of receptors to trigger downstream intracellular signaling, including the canonical Gs/adenylyl cyclase cAMP/protein kinase A (PKA) pathway through the conserved BXXBB and ERW motifs (Johnson and Jonas, 2020; Timossi et al., 2004). Effectively, activation of the cAMP pathway has been recently observed for FSHR and LHR stimulated by pituitary extracts in *S. torazame* (Arimura et al., 2024). In addition, the other conserved motifs could be involved in intracellular trafficking (i.e. export, endocytosis and degradation) *via* the $F(X)_6LL$ motif (Dong et al., 2007), receptor

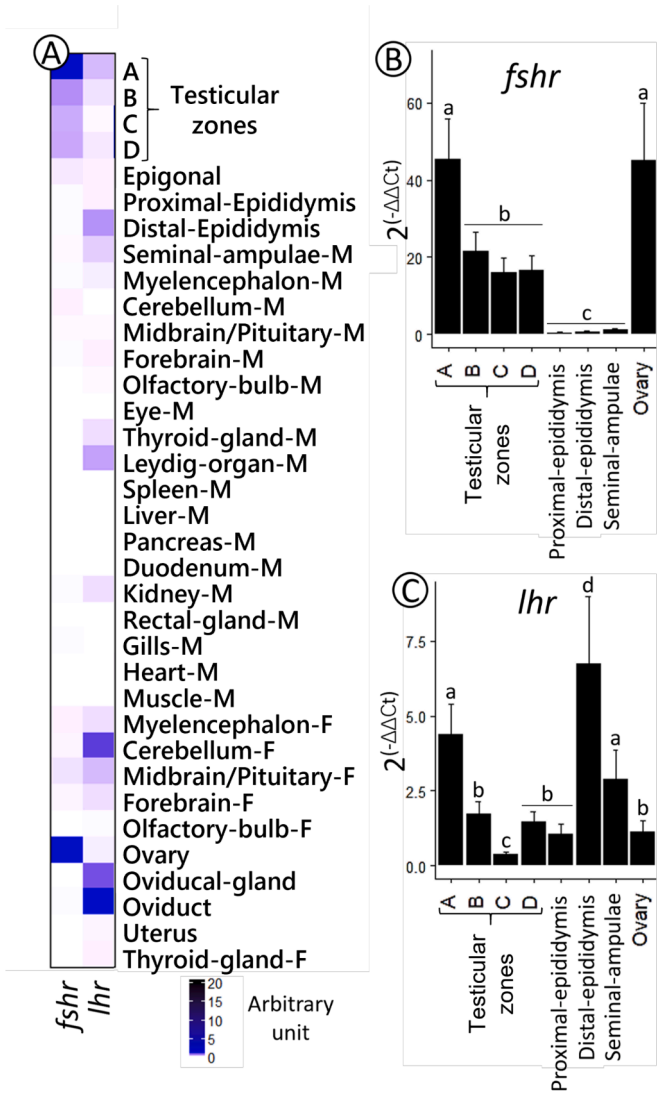

Fig. 4. Relative expression profiles of *fshr* and *lhr* transcripts in *S. canicula* tissues focused on the testis (zones A-D), male genital tract and other male and female tissues. Messenger RNA levels were assayed by real-time PCR. Histology of testicular zones A, B, C and D, corresponding to the zone with spermatogonia, spermatocytes, early spermatids and late spermatids, respectively, is illustrated in Fig. 6. (A) Warm map representation of relative gene expression in 35 different tissues. Relative gene expression of *fshr* (B) and *lhr* (C) along the male genital tract and in the ovary. Statistical analysis was performed using Mann-Whitney *U* test with P value < 0.05 between each statistical groups a, b, c and d. Testicular zones were assayed from six animals in triplicates (N=6; n = 18) and other tissues from three animals in triplicates (N=3; n = 9). The tissues from females corresponded to females caught in September (non-breeding period) whose ovaries contained a few early vitellogenic follicles. M, Male; F, Female.

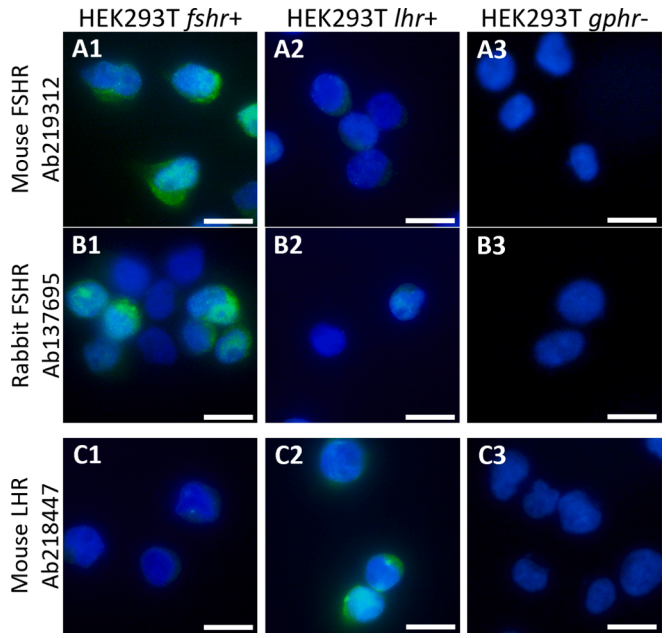

Fig. 5. Immunocytofluorescence on HEK293T cells expressing *S. canicula gthrs*. HEKT293T cells were transfected with pTarget-*scfshr*, pTarget-*sclhr* or empty pTarget plasmids. After 24 h, cells were fixed with 4 % PFA, collected on polysine slides and immunocytofluorescence was performed with mouse monoclonal anti-human FSHR antibody (1:100, ab219312) (A1-A3), rabbit polyclonal anti-human FSHR antibody (1:100, ab137695) (B1-B3) or mouse monoclonal anti-human LHR antibody (1:100, ab218447) (C1-C3). Secondary antibodies used were anti-mouse goat IgI (H+L), Alexa Fluor™ 488 (1:250, A-11001) (A1-A3 and C1-C3) or anti-rabbit goat IgG (H+L) goat antibody, Alexa Fluor™ 488 (1:250, A-11008) (B1-B3). Merged pictures were aquired at 460 nm (DAPI, in blue) and 488 nm (Alexa fluor 488, in green). Scale bars: 5 μm.

desensitization, recycling and G_s-independent ERK1/2-mediated signaling *via* beta-arrestin the class B serine/threonine (S/T) cluster (Kara et al., 2006; Marion et al., 2006; Troispoux et al., 1999; Wehbi et al., 2010).

Ligand-receptor interaction analyses, using transiently transfected HEK293T cells expressing *scfshr* or *sclhr* with the promiscuous *hs*Gα_{16}, showed that *sc*FSHR could be activated either by *sc*FSH or *sc*LH in the same range of efficiency, while *sc*LHR could be only activated by *sc*LH. The EC_{50} obtained ranged from 103 to 383 pM, which is consistent with those obtained with human LH/CGR couples (Riccetti et al., 2017). Moreover, neither of the two receptors, *sc*FSHR and *sc*LHR, was activated by *sc*TSH. Interestingly, the *sc*FSHR could also be activated by *sc*FSH when transiently transfected in mLTC cells. Thus, using two types of *in vitro* functional assays, it appears that *sc*FSHR could be activated by *sc*FSH and cross-activated by *sc*LH while *sc*LHR could only be activated by *sc*LH in HEK293T cells. These results were supported by the similar structure observed between the receptor-binding site of *S canicula* LHβ and that of FSHβ from *S. canicula* and of FSHβ from *H. sapiens*. Cross-activation of FSHR by LH has been also observed in some actinopterygians such as the African catfish (García-López et al., 2009), Atlantic salmon (Andersson et al., 2009) or Japanese eel (Kazeto et al., 2008). However, *sc*LHR is not cross-activated by *sc*FSH, which is similar to the results in the Japanese eel (Suzuki et al., 2020) but differs from observations in zebrafish (Xie et al., 2017) and medaka (Burow et al., 2020) where both FSH and LH were able to activate FSHR or LHR, or in rainbow trout where LHR could be activated by FSH (Sambroni et al., 2007). Furthermore, the ligand-receptor binding results obtained in the catshark also differ from those of *C. milii* where each receptor is activated only by its own ligand (Buechi and Bridgham, 2017). However, the comparison between the two species remains to be investigated since the assays used different detection systems (Ca-signaling in our study, CRE-activity in the study in *C. milii*). In our study, the HEK293T bioassay did not exhibit signal with the cAMP detection system, whereas the mLTC bioassay did when cells were transfected with *scfshr* and stimulated with *sc*FSH or *sc*LH. Unlike HEK293T cells, mLTC cells express endogenous murine LH receptors (mLHR) that are not activated by scLH (Figure S9) but that can potentially dimerize with the transfected *scfshr*. Such a dimerization in mLTCs would favor the cAMP signaling by adequately connecting the sc-FSHR/mLHR dimer with the downstream murine Gs protein. Moreover, in mLTC cells, we use a mix of IBMX, forskolin and oxytocin in the preincubation step which does not modifiy the basal cAMP level but considerably amplifies the cAMP response to GTHs relative to HEK293T cells, allowing detection of much lower

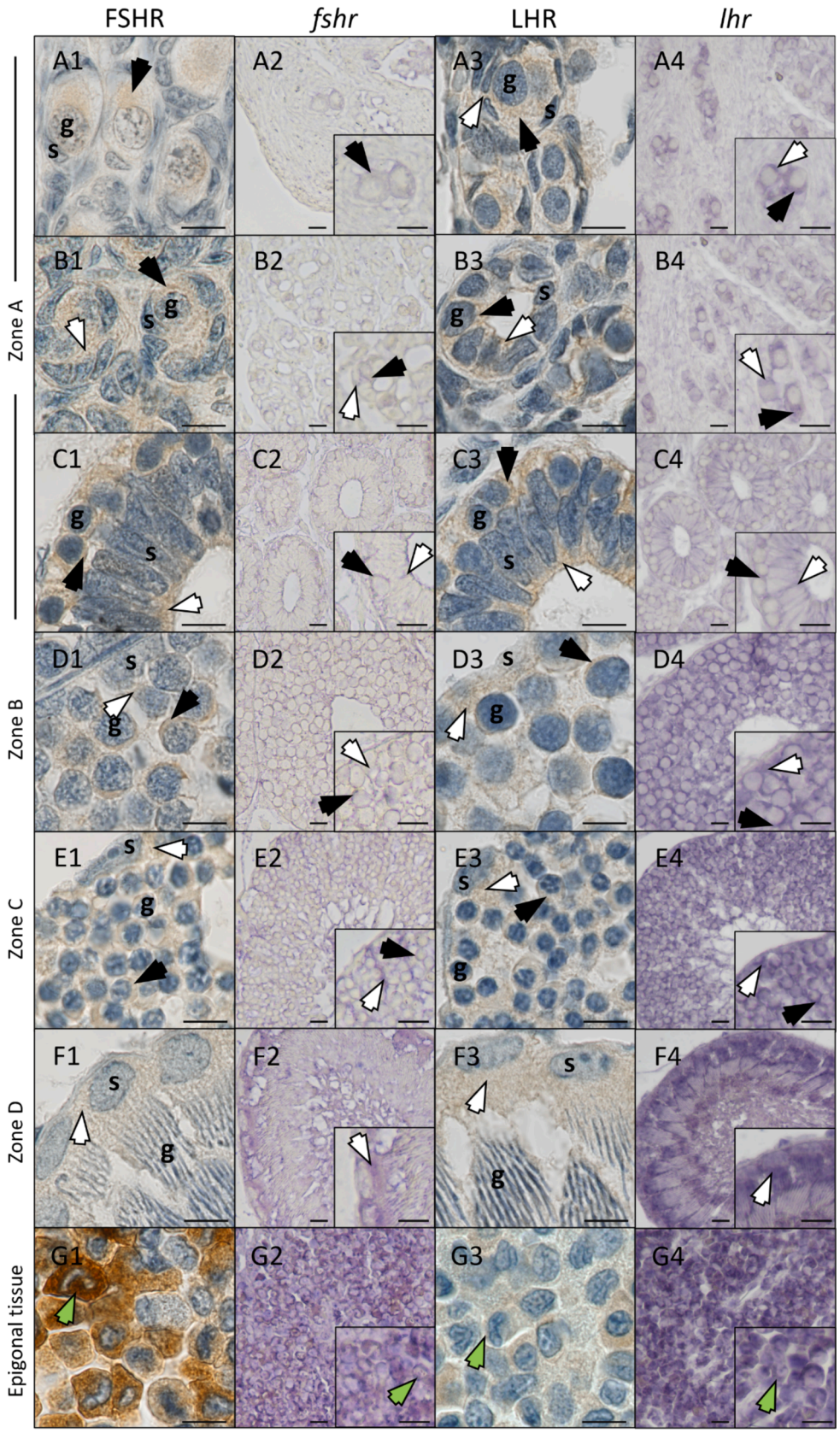

(caption on next page)

Fig. 6. Immunohistochemistry and RNA *in situ* hybridization of GTHRs and *gthrs* in *S. canicula* testicular sections. The testicular zone A corresponds to the germinative area (A1-A4), cysts in formation (B1-B4) and formed cysts with spermatogonia (C1-C4). The testicular zones B, C and D correspond to cysts with primary spermatocytes (D1-D4), cysts with young spermatids (E1-E4) and cysts with late spermatids (F1-F4), respectively. The lymphomyeloid epigonal tissue is illustrated (G1-G4). Immunohistochemistry was performed using rabbit polyclonal anti-human FSHR antibody (ab137695) (A1-G1) and mouse monoclonal anti-human LHR antibody (ab218447) (A3-G3). HRP-tagged secondary antibodies are then detected with DAB substrate kit. *In situ* hybridizations were performed using riboprobes targeting *Sc-fshr* mRNA (A2-G2) or *Sc-lhr* mRNA (A4-G4). For immunostaining and revelation, the DIG-Nucleic Acid Detection Kit was used. Black arrowheads, staining associated with germ cells; white arrowhead, staining associated with somatic precursors (A1-B4) or with Sertoli cells (C1-F4); green arrowhead, staining associated with myelocytes and granulocytes (G1-G4); g, germinal cell nuclei; s, sertolian precursor (A1-B4) or sertolian nuclei (C1-F4). Scale bars: 10 μm. Controls are presented in supplementary data (Fig. S9).

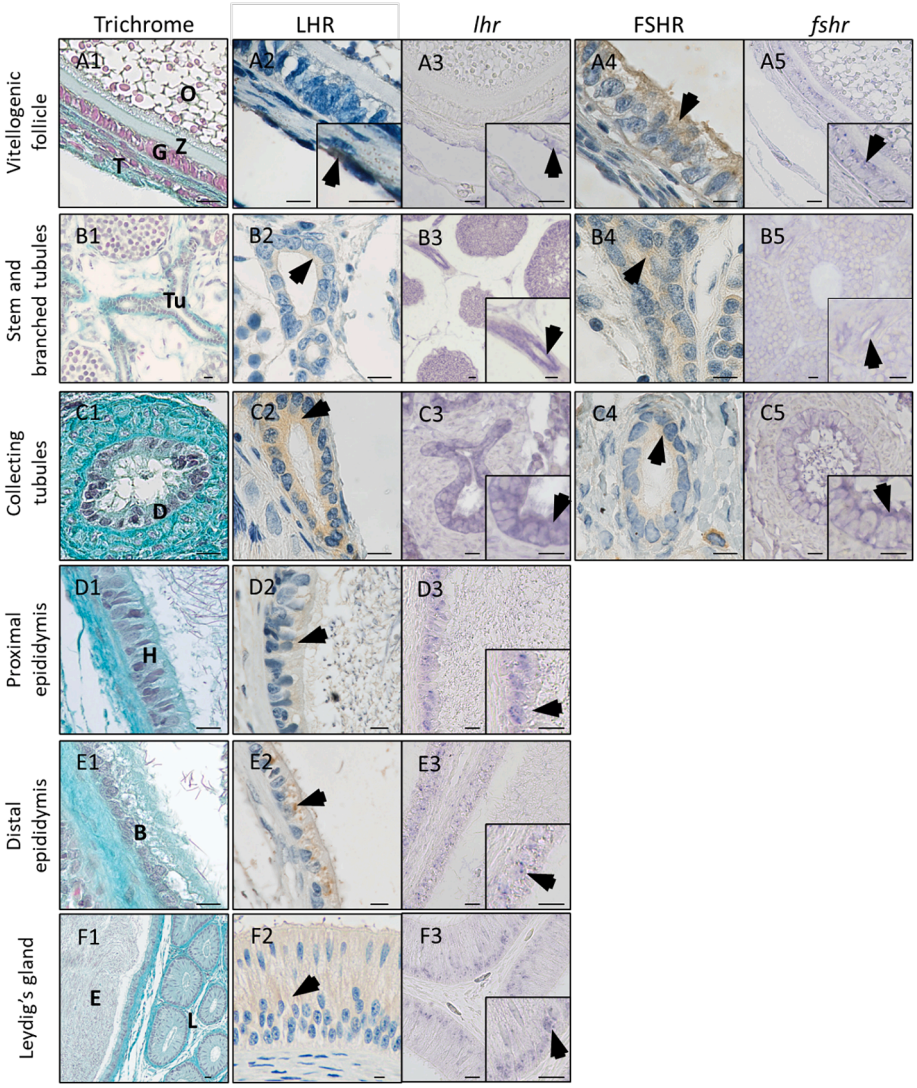

Fig. 7. Immunohistochemistry and RNA *in situ* hybridization of FSHR, LHR, *fshr* and *lhr* in *S. canicula* vitellogenic flollicle sections and other organs associated with the male genital tract. Histology of studied organs is presented (A1-F1) and corresppond to a vitellogenic follicle (A1-A5), intratesticular tubules (B1-B5), testicular collecting tubules (C1-C5), proximal and distal epididymis (D1-E3) and the Leydig's gland adjacent to epididymis (F1-F3). Immunohistochemistry was performed using mouse monoclonal anti-human LHR antibody (ab218447) (A2-F2) or rabbit polyclonal anti-human FSHR antibody (ab137695) (A4-C4). *In situ* hybridizations were performed using riboprobes targeting *fshr* mRNA (A3-F3) or *lhr* mRNA (A5-B5). In the vitellogenic follicle, expressions of LHR/*lhr* and FSHR/*fshr* were observed in theca cells (white arrowhead) and granulosa cells (grey arrowhead), respectively (A2-A5). In the male genital tract, expressions of LHR/*lhr* and FSHR/*fshr* were observed in epithelial cells (black arroheads) of stem and branched tubules (B2-B5), collecting tubules (C2-C5) and expressions of LHR/*lhr* were observed in the epithelial cells of the proximal epididymis (D2-D3), distal epididymis (C2-C3) and of the leydig's gland (F2-F3). T: theca layer; G: granulosa layer; Z: zona pellucida; O: ooplasm; Tu: intratesticular tubules; D: efferent duct; H: epithelium of the proximal epididymis; B: epithelium of the distal epididymis, E: epididymis; L: Leydig's gland D: Scale bars: 10 μm. Controls are presented in supplementary data (Fig. S10).

amounts of gonadotropins. On the other hand, as the functional tests were carried out in heterologous mammalian cells at 37 °C, the specificity of the receptors may be altered and our conclusions should be viewed with this limitation in mind.

From a structural point of view, the LH/FSH specificity, or lack of it, can be interpreted using the "negative specificity" model (Combarnous & Hengé, 1981; Combarnous, 1992) in which the high affinity of gonadotropins is largely due to their common α-subunit (i.e. not specific) whereas their specificities rely on the β-subunit-directed-binding inhibition to each other's receptor. In this model, specificity can be changed

by modifying only a few amino-acid residues in the seatbelt without altering the high affinity towards the receptors. This view is in agreement with easy appearances and disappearances in FSH/LH specificity during Evolution.

4.2. Expressions and functions of gonadotropins

Since the initial purification of a gonadotropic fraction from the ventral lobe of the pituitary (VPD) in *S. canicula* (Sumpter et al., 1978) and the CGα, LHβ, FSHβ identification twenty years later (Quérat et al., 2001), the sequencing of the genomes of several chondrichthyes has allowed major advances in phylogeny of GpHs and their receptors. Orthologs of *cgα*, *lhβ* and *fshβ* have been identified in the genome of the three elasmobranchs *R. typus*, *C. punctatum* and *S. torazame* and are mainly expressed in the VPD for *S. torazame* (Arimura et al., 2024; Hara et al., 2018). In *S. canicula*, although we have not precisely studied their brain localization by *in situ* analyses, our results show the highest expression of *fshβ* and *lhβ* in the midbrain/pituitary of males and females, which agrees with these previous data.

As previously observed in *S. torazame*, *fshr* is mainly expressed in ovaries and testes and *lhr* in ovaries and, surprisingly, in male Leydig organs, but not, or very weakly, in testes (Hara et al., 2018). In our present study, *fshr* and *lhr* are expressed in both gonads of *S. canicula*, but *lhr* is more weakly expressed than *fshr*. During spermatogenesis, the highest *fshr* expression level is associated with early stages where transcripts and proteins are localized in undifferentiated and differentiating spermatogonia. These results are consistent with the expression of FSHR by spermatogonial stem cells, recently demonstrated in humans and mice, which could regulate their differentiation (Bhartiya et al., 2021; Patel and Bhartiya, 2016). In the following stages of spermatogenesis, *fshr* expression decreases and is localized to germ cells and Sertoli cells, consistent with FSH function in supporting meiotic cell survival and spermiogenesis in sarcopterygians and actinopterygians (Huhtaniemi, 2015). With regard to *lhr* expression, higher levels of transcripts have also been found associated with the early stages of spermatogenesis, as for *fshr* mRNA. Here, *lhr* transcripts are apparently expressed by progenitor somatic cells and undifferentiated spermatogonia and could therefore be associated with their differentiation. Then, during the following stages of spermatogenesis, *lhr* expression decreases until the stage of cysts with round spermatids and increases again in the zone containing cysts with late spermatids and is instead associated with differentiated Sertoli cells, for both transcripts and proteins. In mammals, LH regulates the production of steroids by Leydig cells, enabling the completion of meiosis and spermiogenesis (Kumar, 2005; Ramaswamy and Weinbauer, 2014). In actinopterygians, one *fshr* and two *lhr* genes (*lhcgr1* and *lhcgr2*) have been identified (Maugars and Dufour, 2015). FSHR and LHR2 are expressed both in Leydig cells and Sertoli cells, in some species as for example in *Danio rerio*, and both gonadotropins stimulate steroid production (García-López et al., 2010; Ohta et al., 2007; Planas, 1995), with LH being primarily involved in spermiogenesis and spermiation (Chu et al., 2015; Xie et al., 2017). The expression of *fshr* and *lhr* in Sertoli cells of *S. canicula* may be associated with the fact that the main steroid-producing cell is the Sertoli cell in this species, based on its steroidal ultrastructural features and the fact that isolated cysts, as in *S. acanthias,* have the capacity to synthesize androgens in the absence of differentiated Leydig cells (Cuevas et al., 1993; Cuevas and Callard, 1992; Loir et al., 1995; Sourdaine and Garnier, 1993). However, previous studies of the pituitary VPD lobectomy showed no reduction in plasma testosterone concentration, and only total hypophysectomy resulted in a slight drop in testosterone levels, of around 18 % (Dobson and Dodd, 1977a). Similarly, *in vitro* stimulation of steroidogenesis from testicular explants or isolated cysts with VPD extracts or dibutyryl cAMP showed only a 1.5-fold stimulation of testosterone (Sourdaine et al., 1990; Sourdaine and Garnier, 1993). These results suggest that gonadotropic hormones stimulate testicular steroidogenesis to a limited extent. However, ventral lobectomy induces disruption of spermatogenesis at the transition between the last mitosis of spermatogonia and the early stages of primary spermatocytes. This suggests an essential role for gonadotropins for entry into prophase (Dobson and Dodd, 1977b), in agreement with our observation of gonadotropin receptor expression at early stages (zone A).

Furthermore, we observed an unexpected expression of gonadotropin receptors in epigonal tissue. Even if functions of gonadotropins on this tissue remain to be explored, it is of interest to point them out as mammalian hematopoietic progenitors express functional LHR and FSHR and proliferate *in vivo* and *in vitro* in response to gonadotropins and prolactin (Abdelbaset-Ismail et al., 2016; Mierzejewska et al., 2015). In elasmobranchs, functional interactions between gonads and their associated lymphomyeloid epigonal tissue have been previously reported. The epigonal tissue has been described to play a role in cyst resorption after spermiation, to have an inhibitory effect on premeiotic stages DNA synthesis, and to be influenced by gonadal activity and steroids (Lutton and Callard, 2007, 2008; McClusky and Sulikowski, 2014; Piferrer and Callard, 1995).

In the male genital tract, *lhr*, but not *fshr*, is highly expressed in the distal epididymis, with expression localized in epithelial cells, but also in the Leydig's gland, unique to elasmobranchs. In mammals, *lhr* is also expressed in the epididymis of several species such as the rat (Shayu and Rao, 2006) or the squirrel (Wang et al., 2019) and participates in the regulation of the local steroidogenesis (Lei et al., 2001; Wang et al., 2018), resulting in the unique microenvironment necessary for sperm maturation (James et al., 2020; Johnston et al., 2005). Epididymis in elasmobranchs may carry out similar functions, creating a specific microenvironment and being involved in the acquisition of sperm motility (Dzyuba et al., 2019; Jones et al., 1984; Minamikawa' and Morisawa, 1996). Interestingly, a recent study on the stingray *Potamotrygon wallacei* showed the expression of the progesterone receptor in epithelial cells of the epididymis and of the Leydig's gland, with a cell localization quite similar to those we determined for LHR (Morales-Gamba et al., 2023). All these results raise the question of the primitive role of the epididymis and its relationship with internal fertilization, which could be a primitive character of gnathostomes based on the observation of placoderm fossils (Long et al., 2015).

In contrast to the somatic cell composition of the testis in *S. canicula*, where Sertoli cells are differentiated and associated with steroidogenesis, while Leydig cells are rare and undifferentiated, ovarian follicles have differentiated granulosa cells and theca cells forming an inner and outer layer, respectively (Kousteni and Megalofonou, 2020; Lutton et al., 2011). Although the aim of our study was not a detailed study of gonadotropin receptor expression in the ovary, *in situ* analyses did indeed show specific expression of *fshr* and FSHR in the granulosa cells and *lhr* and LHR in theca cells. We also observed that *fshr* expression was higher than that of *lhr* in our sampled ovaries containing previtellogenic follicles and corresponding to postovulatory females. This result is in agreement with results obtained in *S. torazame* (Arimura et al., 2024), where *fshr* was more highly expressed in previtellogenic follicles, while *lhr* expression increased in vitellogenic and maturing follicles. Furthermore, it is interesting to note that *lhr*, but not *fshr,* is highly expressed in the *S. canicula*'s oviduct and oviducal gland whose basic functions are the egg capsule formation, initiated by progesterone in the cloudy catshark, and sperm storage (Marongiu et al., 2021; Shimoyama et al., 2023). Moreover, only *lhr* expression is found in the extragonadal parts of the female tracts, as in the male, underlining the function of LH in these locations.

4.3. Evolution of the gonadal regulation by gonadotropins

Our results can also be discussed in the light of the contribution of data from a chondrichthyan to our understanding of the evolution of gonadal regulation by gonadotropins (Fig. 8). In cyclostomes, reproduction is thought to be regulated by the single glycoprotein hormone GPA2/GpHβ, which activates the GpHRI receptor (Hausken et al., 2018).

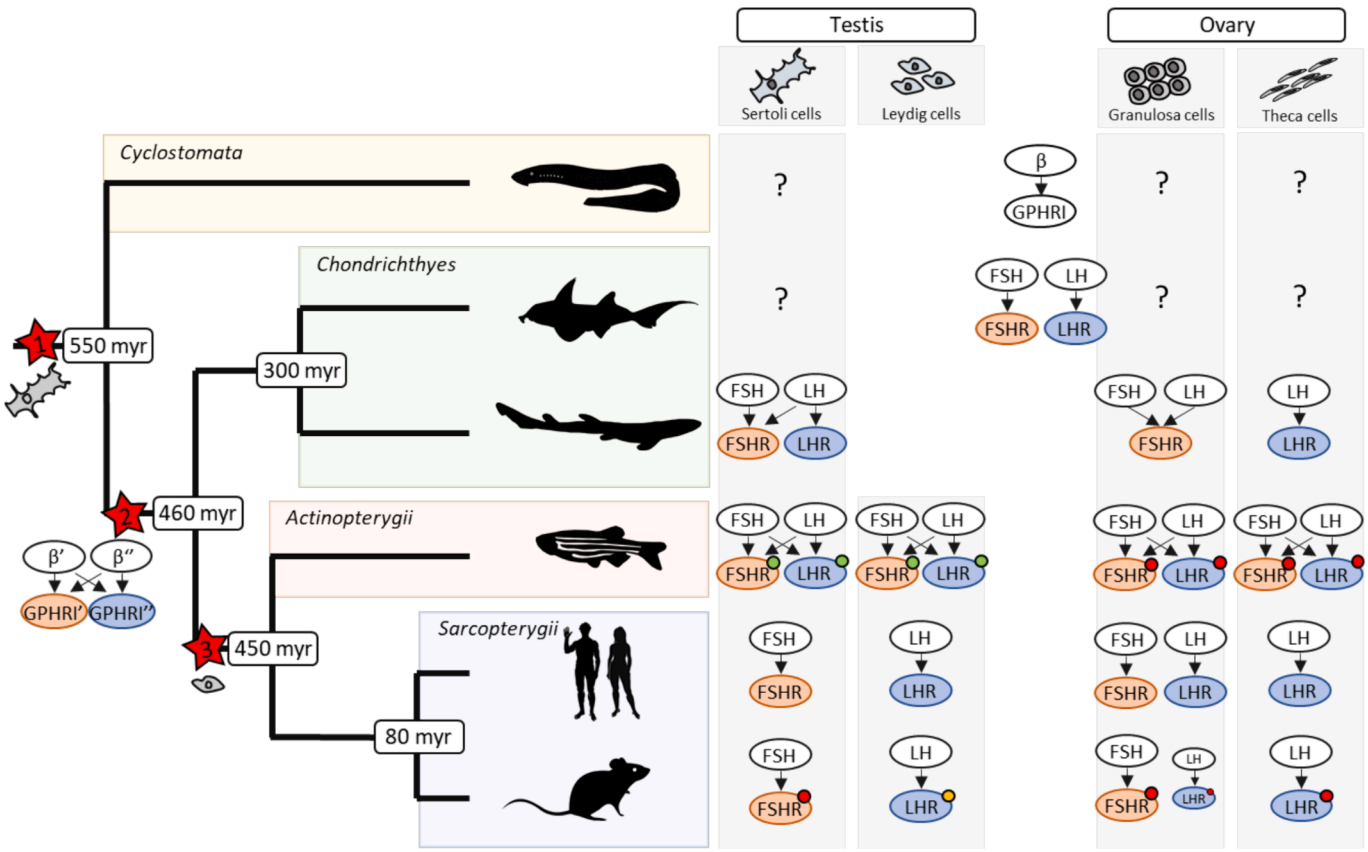

Fig. 8. A proposed analysis of the co-evolution between gonadotropin hormones, their receptors and gonad structures in vertebrates. In cyclostomata, Sertoli cells have been identified and reproduction may be regulated by a single glycoprotein hormone GPA2/GpHβ activating the type I GpHR receptor. In the holocephalan *C. milii*, the two gonadotropins LH and FSH are differentiated, activating their cognate receptors, whose fuctions on gametaogenesis remain unexplored. In elasmobranchs, Sertoli cells are the main steroidogenic cells and functional Leydig cells are present or absent according to species. The present study showed that Sertoli cells express FSHR and LHR, theca cells LHR and Granulosa cells FSHR and that FSHR can be activeted by LH. In actinopterygians, according to species, FSHR and LHR can be expressed by both Leydig and Sertoli cells and FSHR and/or LHR are less discriminating for ligand, and as shown in D. rerio, expression of one of the receptors is sufficient to maintain complete spermatogenesis but not folliculogenesis. In sarcopterygians, Sertoli cells are specifically regulated by FSH, Leydig cells by LH, granulosa cells by FSH (untill maturation where granulosa cells also express LHR), and expression of FSHR alone may be sufficient to maintain spermatogeneis with high testosterone concentrations, but expression of both LHR and FSHR are required to suppport folliculogenesis. In the course of evolution, it could be hypothesized that the first differentiation of functional Sertoli cells was fundamental, while the Leydig cell differentiated later to support Sertoli cell functions with functional redundancy of gonadotropins. About folliculogenesis, cell-specific regulations were established earlier, with functional complementarity of gonadotropins. Green circles, knockout fully fertile; Red circles, knockout infertile; Orange circle, knockout infertile which could be partially compensate with a testosterone treatment; Red star 1, fully functional Sertoli cells; Red star 2, diversification event of ancestral genes encoding subunits of ancestral GTH (name β) and its cognate receptor, prior to GTH specification; Red star 3, fully functional Leydig cells.

In these species Sertoli cells have been previously identified (Engel and Callard, 2007). Distinct LH and FSH have been identified in the holocephalan *C. milii* (Buechi and Bridgham, 2017), but their functions on gametogenesis remain unexplored. Moreover, testicular organization of holocephalans is poorly documented, although Sertoli cells have been mentioned (Stanley et al., 1984), whereas ovarian follicles have been better described and possess, as in other chondrichthyes, granulosa cells and thecae (Díaz Andrade et al., 2018). In elasmobranchs, Sertoli cells are the main cellular site of steroid synthesis, with the contribution of Leydig cells, when present and differentiated according to species (Awruch, 2013; Loir et al., 1995; Prisco et al., 2002; Pudney and Callard, 1984). Sertoli cells therefore appear to be the main cells regulating spermatogenesis, under the control of FSH and LH. In actinopterygian teleosts, FSHR and LHR can be expressed by both Leydig and Sertoli cells, depending on the species, and FSHR and LHR are less discriminating for ligand, except for LHR in the eel, suggesting a functional redundancy of gonadotropins. This has been validated by knock-out approaches in the zebrafish where *lhr;fshr* double-KO males had underdeveloped testes and were infertile (Zhang et al., 2015), but the expression of only FSHR or LHR was sufficient to maintain complete spermatogenesis (Xie et al., 2017). Interestingly, in the medaka, the *lhr* KO, *fshr* KO and *lhr;fshr* double-KO phenotypes presented fertile males with histologically normal testes containing all stages of spermatogenesis and no marked differences in steroid hormone levels (Kitano et al., 2022). Finally, in tetrapods, Sertoli cells are specifically regulated by FSH and Leydig cells by LH, leading to functional complementarity; i.e. separation and complementarity of FSHR-bearing and LHR-bearing cells. This was also further supported by knock-out approaches showing that FSHR-KO or LHR-KO mice were infertile due to absent sertolian or leydigian functions, respectively (Oduwole et al., 2021; Pakarainen et al., 2005). But in the case of the LHR KO mice, strong FSH stimulation can maintain spermatogenesis without LH and high testosterone concentration, thus highlighting the central role of the Sertoli cells and the more marginal role of the Leydig cells (Oduwole et al., 2021; Pakarainen et al., 2005).

In conclusion, we postulate that during vertebrate evolution, the differentiation of functional Sertoli cells preceded that of the Leydig cell which essentially backed the Sertoli cell functions. Sertoli cells were initially regulated by a single gonadotropin, as in cyclostomes, before LH and FSH differentiated in chondrichthyans, and their receptors

expressed in different cells in most bony vertebrates, except in some actinopterygians. Regarding folliculogenesis, the differentiation of granulosa and theca cells must have appeared before the divergence of cyclostomes and the differentiation of FSHR and LHR (Dziewulska and Domagala, 2009). But, once differentiated, both gonadotropins were necessary for functional folliculogenesis in gnathostomes (Chu et al., 2015; Murozumi et al., 2014; Oduwole et al., 2021; Xie et al., 2017). Overall, this suggests that folliculogenesis requires more specific regulation, than spermatogenesis, with the emergence of the two gonadotropins to meet the needs of ovarian development and function, as previously hypothesized (Xie et al., 2017).

Funding

This work was supported by the "Ministère de l'Enseignement Supérieur et de la Recherche Scientifique" [F.J.'s PhD grant]; the European Regional Development Fund under the project "Manche 2021 – Plateformes d'exploitation de ressources marines" [Operational Program ERDF/ESF 2014–2020]; the "Région Normandie" under the project "Emergent – CauSy" [grant number 22E02935/00126108]; the GIS FC3R on funds operated by Inserm (France) [grant number 22FC3R-008].

CRediT authorship contribution statement

Fabian Jeanne: Writing – review & editing, Writing – original draft, Resources, Methodology, Investigation, Formal analysis, Data curation, Conceptualization. **Stanislas Pilet:** Resources, Methodology, Investigation, Formal analysis. **Danièle Klett:** Writing – review & editing, Resources, Methodology, Investigation, Funding acquisition, Formal analysis, Data curation, Conceptualization. **Yves Combarnous:** Writing – review & editing, Resources, Methodology, Investigation, Funding acquisition, Formal analysis, Data curation, Conceptualization. **Benoît Bernay:** Writing – review & editing, Resources, Methodology, Investigation, Formal analysis, Data curation, Conceptualization. **Sylvie Dufour:** Writing – review & editing, Investigation, Formal analysis. **Pascal Favrel:** Writing – review & editing, Supervision, Resources, Project administration, Methodology, Investigation, Funding acquisition, Formal analysis, Data curation, Conceptualization. **Pascal Sourdaine:** Writing – review & editing, Supervision, Resources, Project administration, Methodology, Investigation, Funding acquisition, Formal analysis, Data curation, Conceptualization.

Declaration of Competing Interest

The authors declare that they have no known competing financial interests or personal relationships that could have appeared to influence the work reported in this paper.

Data availability

Data is provided as supplementary file

Acknowledgments

The authors are grateful to the European Regional Development Fund, Inserm (France), the *Ministère de l'Enseignement Supérieur et de la Recherche Scientifique*, the *Région Normandie and Inserm (France) for fundings*, Didier Leroy from the CGFS (Channel Ground Fish Survey) campaign (IFREMER in the East Manche in September 2022) for providing the catsharks, and to Frédérique Guyon of the "Centre de Recherches en Environnement Côtier" (Luc sur Mer, France) for the care given to the animals.

Appendix A. Supplementary data

Supplementary data to this article can be found online at https://doi.org/10.1016/j.ygcen.2024.114614.

References

Abdelbaset-Ismail, A., Suszynska, M., Borkowska, S., Adamiak, M., Ratajczak, J., Kucia, M., Ratajczak, M.Z., 2016. Human haematopoietic stem/progenitor cells express several functional sex hormone receptors. Journal of Cellular and Molecular Medicine 20, 134–146. https://doi.org/10.1111/jcmm.12712.

Andersson, E., Nijenhuis, W., Male, R., Swanson, P., Bogerd, J., Taranger, G.L., Schulz, R. W., 2009. Pharmacological characterization, localization and quantification of expression of gonadotropin receptors in Atlantic salmon (Salmo salar L.) ovaries. General and Comparative Endocrinology 163, 329–339. https://doi.org/10.1016/j.ygcen.2009.05.001.

Arimura, S., Wong, M.K.S., Inoue, R., Kawano, M., Shimoyama, K., Fujimori, C., Tokunaga, K., Takagi, W., Hyodo, S., 2024. Functional characterization of follicle-stimulating hormone and luteinizing hormone receptors in cloudy catshark. Scyliorhinus Torazame. General and Comparative Endocrinology 354, 114542. https://doi.org/10.1016/j.ygcen.2024.114542.

Awruch, C.A., 2013. Reproductive endocrinology in chondrichthyans: The present and the future. General and Comparative Endocrinology 192, 60–70. https://doi.org/10.1016/j.ygcen.2013.05.021.

Belghazi, M., Klett, D., Cahoreau, C., Combarnous, Y., 2006. Nitro-thiocyanobenzoic acid (NTCB) reactivity of cysteines beta100 and beta110 in porcine luteinizing hormone: metastability and hypothetical isomerization of the two disulfide bridges of its beta-subunit seatbelt. Mol Cell Endocrinol. 247, 175–182. https://doi.org/10.1016/j.mce.2006.01.001.

Bhartiya, D., Patel, H., Kaushik, A., Singh, P., Sharma, D., 2021. Endogenous, tissue-resident stem/progenitor cells in gonads and bone marrow express FSHR and respond to FSH via FSHR-3. J Ovarian Res 14, 145. https://doi.org/10.1186/s13048-021-00883-0.

Bosseboeuf, A., Gautier, A., Auvray, P., Mazan, S., Sourdaine, P., 2014. Characterization of spermatogonial markers in the mature testis of the dogfish (Scyliorhinus canicula L.). REPRODUCTION 147, 125–139. https://doi.org/10.1530/REP-13-0316.

Buechi, H.B., Bridgham, J.T., 2017. Evolution of specificity in cartilaginous fish glycoprotein hormones and receptors. General and Comparative Endocrinology 246, 309–320. https://doi.org/10.1016/j.ygcen.2017.01.007.

Burova, T., Lecompte, F., Galet, C., Monsallier, F., Delpech, S., Haertlé, T., Combarnous, Y., 2001. Conformational stability and in vitro bioactivity of porcine luteinizing hormone. Mol Cell Endocrinol. 176, 129–134. https://doi.org/10.1016/S0303-7207(01)00447-6.

Burow, S., Mizrahi, N., Maugars, G., Von Krogh, K., Nourizadeh-Lillabadi, R., Hollander-Cohen, L., Shpilman, M., Atre, I., Weltzien, F.-A., Levavi-Sivan, B., 2020. Characterization of gonadotropin receptors Fshr and Lhr in Japanese medaka. Oryzias Latipes. General and Comparative Endocrinology 285, 113276. https://doi.org/10.1016/j.ygcen.2019.113276.

Callard, G.V., 1991. Reproduction in male elasmobranch fishes. In: Kinne, R.K.H., Kinne-Saffran, E., Beyenbach, K.W. (Eds.), Oogenesis, Spermatogenesis and Reproduction. Karger, Basel, pp. 104–154.

Campbell, R., 2004. Piecing together evolution of the vertebrate endocrine system. Trends in Genetics 20, 359–366. https://doi.org/10.1016/j.tig.2004.06.005.

Chauvigné, F., Tingaud-Sequeira, A., Agulleiro, M.J., Calusinska, M., Gómez, A., Finn, R. N., Cerdà, J., 2010. Functional and Evolutionary Analysis of Flatfish Gonadotropin Receptors Reveals Cladal- and Lineage-Level Divergence of the Teleost Glycoprotein Receptor Family. Biology of Reproduction 82, 1088–1102. https://doi.org/10.1095/biolreprod.109.082289.

Chu, L., Li, J., Liu, Y., Cheng, C.H.K., 2015. Gonadotropin Signaling in Zebrafish Ovary and Testis Development: Insights From Gene Knockout Study. Molecular Endocrinology 29, 1743–1758. https://doi.org/10.1210/me.2015-1126.

Cuevas, M.E., Callard, G., 1992. In vitro steroid secretion by staged spermatocysts (sertoli/germ cell units) of dogfish (Squalus acanthias) testis. General and Comparative Endocrinology 88, 151–165. https://doi.org/10.1016/0016-6480(92)90204-W.

Cuevas, M.E., Collins, K., Callard, G.V., 1993. Stage-related changes in steroid-converting enzyme activities in Squalus testis: synthesis of biologically active metabolites via 3b-hydroxysteroid dehydrogenase/ isomerase and 5a-reductase. Steroids 58, 87–94. https://doi.org/10.1016/0039-128X(93)90058-U.

Díaz Andrade, M.C., Moya, A.C., Wehitt, A., Di Giácomo, E.E., Galíndez, E.J., 2018. Observations of follicle cell processes in a holocephalan. Journal of Fish Biology 93, 424–427. https://doi.org/10.1111/jfb.13736.

Dobson, S., Dodd, J.M., 1977a. Endocrine control of the testis in the dogfish Scyliorhinus canicula L. I. Effects of partial hypophysectomy on gravimetric, hormonal and biochemical aspects of testis function. General and Comparative Endocrinology 32, 41–52. https://doi.org/10.1016/0016-6480(77)90081-8.

Dobson, S., Dodd, J.M., 1977b. The roles of temperature and photoperiod in the response of the testis of the dogfish, Scyliorhinus canicula L. to partial hypophysectomy (ventral lobectomy). General and Comparative Endocrinology 32, 114–115. https://doi.org/10.1016/0016-6480(77)90088-0.

Dong, C., Filipeanu, C.M., Duvernay, M.T., Wu, G., 2007. Regulation of G protein-coupled receptor export trafficking. Biochimica et Biophysica Acta (BBA) - Biomembranes 1768, 853–870. doi: 10.1016/j.bbamem.2006.09.008.

Duan, J., Xu, P., Cheng, X., Mao, C., Croll, T., He, X., Shi, J., Luan, X., Yin, W., You, E., Liu, Q., Zhang, S., Jiang, H., Zhang, Y., Jiang, Y., Xu, H.E., 2021. Structures of full-length glycoprotein hormone receptor signalling complexes. Nature 598, 688–692. https://doi.org/10.1038/s41586-021-03924-2.

Dufour, S., Quérat, B., Tostivint, H., Pasqualini, C., Vaudry, H., Rousseau, K., 2020. Origin and Evolution of the Neuroendocrine Control of Reproduction in Vertebrates, With Special Focus on Genome and Gene Duplications. Physiological Reviews 100, 869–943. https://doi.org/10.1152/physrev.00009.2019.

Dziewulska, K., Domagala, J., 2009. Ripening of the oocyte of the river lamprey (Lampetra fluviatilis L.) after river entry. Journal of Applied Ichthyology 25, 752–756. https://doi.org/10.1111/j.1439-0426.2009.01325.x.

Dzyuba, V., Ninhaus-Silveira, A., Kahanec, M., Veríssimo-Silveira, R., 2019. Sperm motility in ocellate river stingrays: Evidence for post-testicular sperm maturation and capacitation in chondrichthyes. Journal of Zoology 307, 9–16. https://doi.org/10.1111/jzo.12610.

Engel, K.B., Callard, G.V., 2007. Endocrinology of Leydig Cells in Nonmammalian Vertebrates. In: Payne, A.H., Hardy, M.P. (Eds.), The Leydig Cell in Health and Disease, Contemporary Endocrinology. Humana Press, Totowa, NJ, pp. 207–224. https://doi.org/10.1007/978-1-59745-453-7_15.

Galet, C., Lecompte, F., Combarnous, Y., 2004. Association/dissociation of gonadotropin subunits involves disulfide bridge disruption which is influenced by carbohydrate moiety. Biochem Biophys Res Commun. 324, 868–873. https://doi.org/10.1016/j.bbrc.2004.09.143.

García-López, Á., Bogerd, J., Granneman, J.C.M., Van Dijk, W., Trant, J.M., Taranger, G. L., Schulz, R.W., 2009. Leydig Cells Express Follicle-Stimulating Hormone Receptors in African Catfish. Endocrinology 150, 357–365. https://doi.org/10.1210/en.2008-0447.

García-López, Á., De Jonge, H., Nóbrega, R.H., De Waal, P.P., Van Dijk, W., Hemrika, W., Taranger, G.L., Bogerd, J., Schulz, R.W., 2010. Studies in Zebrafish Reveal Unusual Cellular Expression Patterns of Gonadotropin Receptor Messenger Ribonucleic Acids in the Testis and Unexpected Functional Differentiation of the Gonadotropins. Endocrinology 151, 2349–2360. https://doi.org/10.1210/en.2009-1227.

Gautier, A., Bosseboeuf, A., Auvray, P., Sourdaine, P., 2014. Maintenance of Potential Spermatogonial Stem Cells In Vitro by GDNF Treatment in a Chondrichthyan Model (Scyliorhinus canicula L.). Biology of Reproduction 91, 91–105. https://doi.org/10.1095/biolreprod.113.116020.

Gautron, J., 1978. Effet du calcium et de la stimulation sur les terminaisons nerveuses des fonctions nerf-électroplaque de la Torpille. Biol. Cell. 31, 31–44.

Giraldo, C., Le Roy, D., Martin-Baillet, V., 2022. CGFS2022 cruise. RV Thalassa. https://doi.org/10.17600/18001842.

Hara, Y., Yamaguchi, K., Onimaru, K., Kadota, M., Koyanagi, M., Keeley, S.D., Tatsumi, K., Tanaka, K., Motone, F., Kageyama, Y., Nozu, R., Adachi, N., Nishimura, O., Nakagawa, R., Tanegashima, C., Kiyatake, I., Matsumoto, R., Murakumo, K., Nishida, K., Terakita, A., Kuratani, S., Sato, K., Hyodo, S., Kuraku, S., 2018. Shark genomes provide insights into elasmobranch evolution and the origin of vertebrates. Nat Ecol Evol 2, 1761–1771. https://doi.org/10.1038/s41559-018-0673-5.

Hausken, K.N., Tizon, B., Shpilman, M., Barton, S., Decatur, W., Plachetzki, D., Kavanaugh, S., Ul-Hasan, S., Levavi-Sivan, B., Sower, S.A., 2018. Cloning and characterization of a second lamprey pituitary glycoprotein hormone, thyrostimulin (GpA2/GpB5). General and Comparative Endocrinology 264, 16–27. https://doi.org/10.1016/j.ygcen.2018.04.010.

Helenius, A., Aebi, M., 2004. Roles of N-Linked Glycans in the Endoplasmic Reticulum. Annu. Rev. Biochem. 73, 1019–1049. https://doi.org/10.1146/annurev.biochem.73.011303.073752.

Heyland, A., Plachetzki, D., Donelly, E., Gunaratne, D., Bobkova, Y., Jacobson, J., Kohn, A.B., Moroz, L.L., 2012. Distinct Expression Patterns of Glycoprotein Hormone Subunits in the Lophotrochozoan Aplysia: Implications for the Evolution of Neuroendocrine Systems in Animals. Endocrinology 153, 5440–5451. https://doi.org/10.1210/en.2012-1677.

Hiro'oka, T., Maassen, D., Berger, P., Boime, I., 2000. Disulfide Bond Mutations in Follicle-Stimulating Hormone Result in Uncoupling of Biological Activity from Intracellular Behavior. Endocrinology 141, 4751–4756. https://doi.org/10.1210/endo.141.12.7821.

Hsueh, A.J.W., Feng, Y., 2020. Discovery of polypeptide ligand-receptor pairs based on their co-evolution. FASEB J. 34, 8824–8832. https://doi.org/10.1096/fj.202000779R.

Hsueh, A.J., He, J., 2018. Gonadotropins and their receptors: coevolution, genetic variants, receptor imaging, and functional antagonists. Biology of Reproduction 99, 3–12. https://doi.org/10.1093/biolre/ioy012.

Huhtaniemi, I., 2015. A short evolutionary history of FSH-stimulated spermatogenesis. Hormones (athens) 14, 468–478. https://doi.org/10.14310/horm.2002.1632.

Irisarri, I., Baurain, D., Brinkmann, H., Delsuc, F., Sire, J.-Y., Kupfer, A., Petersen, J., Jarek, M., Meyer, A., Vences, M., Philippe, H., 2017. Phylotranscriptomic consolidation of the jawed vertebrate timetree. Nat Ecol Evol 1, 1370–1378. https://doi.org/10.1038/s41559-017-0240-5.

James, E.R., Carrell, D.T., Aston, K.I., Jenkins, T.G., Yeste, M., Salas-Huetos, A., 2020. The Role of the Epididymis and the Contribution of Epididymosomes to Mammalian Reproduction. IJMS 21, 5377. https://doi.org/10.3390/ijms21155377.

Jiang, X., Dias, J.A., He, X., 2014a. Structural biology of glycoprotein hormones and their receptors: Insights to signaling. Molecular and Cellular Endocrinology 382, 424–451. https://doi.org/10.1016/j.mce.2013.08.021.

Jiang, X., Fischer, D., Chen, X., McKenna, S.D., Liu, H., Sriraman, V., Yu, H.N., Goutopoulos, A., Arkinstall, S., He, X., 2014b. Evidence for Follicle-stimulating Hormone Receptor as a Functional Trimer. Journal of Biological Chemistry 289, 14273–14282. https://doi.org/10.1074/jbc.M114.549592.

Johansson, M.U., Zoete, V., Michielin, O., Guex, N., 2012. Defining and searching for structural motifs using DeepView/Swiss-PdbViewer. BMC Bioinformatics 13, 1–11. https://doi.org/10.1186/1471-2105-13-173.

Johnson, G.P., Jonas, K.C., 2020. Mechanistic insight into how gonadotropin hormone receptor complexes direct signaling†. Biology of Reproduction 102, 773–783. https://doi.org/10.1093/biolre/ioz228.

Johnston, D.S., Jelinsky, S.A., Bang, H.J., DiCandeloro, P., Wilson, E., Kopf, G.S., Turner, T.T., 2005. The Mouse Epididymal Transcriptome: Transcriptional Profiling of Segmental Gene Expression in the Epididymis. Biology of Reproduction 73, 404–413. https://doi.org/10.1095/biolreprod.105.039719.

Jones, R.C., Jones, N., Djakiew, D., 1984. Luminal composition and maturation of spermatozoa in the male genital ducts of the Port Jackson shark, *Heterodontus portusjacksoni*. J. Exp. Zool. 230, 417–426. https://doi.org/10.1002/jez.1402300311.

Kara, E., Crépieux, P., Gauthier, C., Martinat, N., Piketty, V., Guillou, F., Reiter, E., 2006. A Phosphorylation Cluster of Five Serine and Threonine Residues in the C-Terminus of the Follicle-Stimulating Hormone Receptor Is Important for Desensitization But Not for β-Arrestin-Mediated ERK Activation. Molecular Endocrinology 20, 3014–3026. https://doi.org/10.1210/me.2006-0098.

Kazeto, Y., Kohara, M., Miura, T., Miura, C., Yamaguchi, S., Trant, J.M., Adachi, S., Yamauchi, K., 2008. Japanese Eel Follicle-Stimulating Hormone (Fsh) and Luteinizing Hormone (Lh): Production of Biologically Active Recombinant Fsh and Lh by Drosophila S2 Cells and Their Differential Actions on the Reproductive Biology. Biology of Reproduction 79, 938–946. https://doi.org/10.1095/biolreprod.108.070052.

Kitano, T., Takenaka, T., Takagi, H., Yoshiura, Y., Kazeto, Y., Hirai, T., Mukai, K., Nozu, R., 2022. Roles of Gonadotropin Receptors in Sexual Development of Medaka.

Klett, D., Combarnous, Y., 2021. Highly sensitive in vitro bioassay for luteinizing hormone and chorionic gonadotropin allowing their measurement in plasma. Reproduction and Fertility 2, 300–307. https://doi.org/10.1530/RAF-21-0045.

Kousteni, V., Megalofonou, P., 2020. Reproductive strategy of Scyliorhinus canicula (L., 1758): a holistic approach based on macroscopic measurements and microscopic observations of the reproductive organs. Mar. Freshwater Res. 71, 596. https://doi.org/10.1071/MF18474.

Kudo, M., Chen, T., Nakabayashi, K., Hsu, S.Y., Hsueh, A.J.W., 2000. The Nematode Leucine-Rich Repeat-Containing, G Protein-Coupled Receptor (LGR) Protein Homologous to Vertebrate Gonadotropin and Thyrotropin Receptors is Constitutively Activated in. Mammalian Cells 14, 272–284. https://doi.org/10.1210/mend.14.2.0422.

Kumar, T.R., 2005. What have we learned about gonadotropin function from gonadotropin subunit and receptor knockout mice? Reproduction 130, 293–302. https://doi.org/10.1530/rep.1.00660.

Lapthorn, A., Harris, D.C., Littlejohn, A., Lustbader, J.W., Canfield, R.E., Machin, K.J., Morgan, F.J., Isaacs, N.W., 1994. Crystal structure of human chorionic gonadotropin. Nature 369, 455–461. https://doi.org/10.1038/369455a0.

Lei, Z.M., Mishra, S., Zou, W., Xu, B., Foltz, M., Li, X., Rao, C.V., 2001. Targeted Disruption of Luteinizing Hormone/Human Chorionic Gonadotropin Receptor Gene. Molecular Endocrinology 15, 184–200. https://doi.org/10.1210/mend.15.1.0586.

Lemoine, F., Correia, D., Lefort, V., Doppelt-Azeroual, O., Mareuil, F., Cohen-Boulakia, S., Gascuel, O., 2019. NGPhylogeny.fr: new generation phylogenetic services for non-specialists. Nucleic Acids Research 47, 260–265. https://doi.org/10.1093/nar/gkz303.

Letunic, I., Bork, P., 2021. Interactive Tree Of Life (iTOL) v5: an online tool for phylogenetic tree display and annotation. Nucleic Acids Research 49, 293–296. https://doi.org/10.1093/nar/gkab301.

Livak, K.J., Schmittgen, T.D., 2001. Analysis of Relative Gene Expression Data Using Real-Time Quantitative PCR and the $2^{-\Delta\Delta CT}$ Method. Methods 25, 402–408. https://doi.org/10.1006/meth.2001.1262.

Loir, M., Sourdaine, P., 1994. Testes cells: isolation and culture. In: Hochachka, P.W., Mommsen, T.P. (Eds.), Biochemistry and Molecular Biology of Fishes: Analytical Techniques. Elsevier, New York, pp. 219–272. https://doi.org/10.1016/B978-0-444-82033-4.50028-3.

Loir, M., Sourdaine, P., Mendis-Handagama, S.M.L.C., Jégou, B., 1995. Cell-cell interactions in the testis of teleosts and elasmobranchs: CELL-CELL INTERACTIONS IN THE TESTIS. Microsc. Res. Tech. 32, 533–552. https://doi.org/10.1002/jemt.1070320606.

Long, J.A., Mark-Kurik, E., Johanson, Z., Lee, M.S.Y., Young, G.C., Min, Z., Ahlberg, P.E., Newman, M., Jones, R., Blaauwen, J.D., Choo, B., Trinajstic, K., 2015. Copulation in antiarch placoderms and the origin of gnathostome internal fertilization. Nature 517, 196–199. https://doi.org/10.1038/nature13825.

Loppion, G., Crespel, A., Martinez, A.-S., Auvray, P., Sourdaine, P., 2008. Study of the potential spermatogonial stem cell compartment in dogfish testis, Scyliorhinus canicula L. Cell and Tissue Research 332, 533–542. https://doi.org/10.1007/s00441-008-0590-z.

Lutton, B.V., Callard, I.P., 2007. Effects of reproductive activity and sex hormones on apoptosis in the epigonal organ of the skate (Leucoraja erinacea). General and Comparative Endocrinology 154, 75–84. https://doi.org/10.1016/j.ygcen.2007.06.014.

Lutton, B.V., Callard, I.P., 2008. Influence of reproductive activity, sex steroids, and seasonality on epigonal organ cellular proliferation in the skate (Leucoraja erinacea). General and Comparative Endocrinology 155, 116–125. https://doi.org/10.1016/j.ygcen.2007.03.011.

Lutton, B.V., George, J.S., Murrin, C.R., Fileti, L.A., Callard, I.P., 2011. The elasmobranch ovary. In: Hamlett, W.C. (Ed.), Reproductive Biology and Phylogeny of Chondrichthyes: Sharks, Batoids, and Chimaeras. SciencePublisher Inc, Einfeld, pp. 237–281.

Manca, R., Glomski, C., Pica, A., 2019. Hematopoietic stem cells debut in embryonic lymphomyeloid tissues of elasmobranchs. European Journal of Histochemistry 63. https://doi.org/10.4081/ejh.2019.3060.

Marion, S., Oakley, R.H., Kim, K.-M., Caron, M.G., Barak, L.S., 2006. A β-Arrestin Binding Determinant Common to the Second Intracellular Loops of Rhodopsin Family G Protein-coupled Receptors. Journal of Biological Chemistry 281, 2932–2938. https://doi.org/10.1074/jbc.M508074200.

Marongiu, M.F., Porcu, C., Pascale, N., Bellodi, A., Cau, A., Mulas, A., Pesci, P., Porceddu, R., Follesa, M.C., 2021. A Taxonomic Survey of Female Oviducal Glands in Chondrichthyes: A Comparative Overview of Microanatomy in the Two Reproductive Modes. Animals 11, 2653. https://doi.org/10.3390/ani11092653.

Marra, N.J., Stanhope, M.J., Jue, N.K., Wang, M., Sun, Q., Pavinski Bitar, P., Richards, V. P., Komissarov, A., Rayko, M., Kliver, S., Stanhope, B.J., Winkler, C., O'Brien, S.J., Antunes, A., Jorgensen, S., Shivji, M.S., 2019. White shark genome reveals ancient elasmobranch adaptations associated with wound healing and the maintenance of genome stability. Proceedings of the National Academy of Sciences 116, 4446–4455. https://doi.org/10.1073/pnas.1819778116.

Maston, G.A., Ruvolo, M., 2002. Chorionic Gonadotropin Has a Recent Origin Within Primates and an Evolutionary History of Selection. Molecular Biology and Evolution 19, 320–335. https://doi.org/10.1093/oxfordjournals.molbev.a004085.

Maugars, G., Dufour, S., 2015. Demonstration of the Coexistence of Duplicated LH Receptors in Teleosts, and Their Origin in Ancestral Actinopterygians. PLoS ONE 10, e0135184.

Maugars, G., Dufour, S., Cohen-Tannoudji, J., Quérat, B., 2014. Multiple Thyrotropin β-Subunit and Thyrotropin Receptor-Related Genes Arose during Vertebrate Evolution. PLoS ONE 9, e111361.

McClusky, L.M., Sulikowski, J., 2014. The epigonal organ and mature pole of the testis in the recreationally fished blue shark (Prionace glauca): histochemico-functional correlates. Journal of Anatomy 225, 614–624. https://doi.org/10.1111/joa.12242.

Mierzejewska, K., Borkowska, S., Suszynska, E., Suszynska, M., Poniewierska-Baran, A., Maj, M., Pedziwiatr, D., Adamiak, M., Abdel-Latif, A., Kakar, S.S., Ratajczak, J., Kucia, M., Ratajczak, M.Z., 2015. Hematopoietic Stem/Progenitor Cells Express Several Functional Sex Hormone Receptors—Novel Evidence for a Potential Developmental Link Between Hematopoiesis and Primordial Germ Cells. Stem Cells and Development 24, 927–937. https://doi.org/10.1089/scd.2014.0546.

Minamikawa', S., Morisawa, M., 1996. Acquisition, Initiation and Maintenance of Sperm Motility in the Shark, Ttiakis scyllia. Comp Biochem Physiol A Mol Integr Physiol 113, 387–392. https://doi.org/10.1016/0300-9629(95)02080-2.

Morales-Gamba, R.D., Araújo, M.L.G., Barcellos, J.F.M., Rêgo, M.G., Dias, L.C., Marcon, J.L., 2023. Progesterone receptors in extratesticular ducts of the Amazonian stingray Potamotrygon wallacei: A potential role in sperm maturation and aggregate formation. General and Comparative Endocrinology 344, 114375. https://doi.org/10.1016/j.ygcen.2023.114375.

Murozumi, N., Nakashima, R., Hirai, T., Kamei, Y., Ishikawa-Fujiwara, T., Todo, T., Kitano, T., 2014. Loss of Follicle-Stimulating Hormone Receptor Function Causes Masculinization and Suppression of Ovarian Development in Genetically Female Medaka. Endocrinology 155, 3136–3145. https://doi.org/10.1210/en.2013-2060.

Nechamen, C.A., Thomas, R.M., Dias, J.A., 2007. APPL1, APPL2, Akt2 and FOXO1a interact with FSHR in a potential signaling complex. Molecular and Cellular Endocrinology 260, 93–99. https://doi.org/10.1016/j.mce.2006.08.014.

Oduwole, O.O., Huhtaniemi, I.T., Misrahi, M., 2021. The Roles of Luteinizing Hormone, Follicle-Stimulating Hormone and Testosterone in Spermatogenesis and Folliculogenesis Revisited. IJMS 22, 12735. https://doi.org/10.3390/ijms222312735.

Ohta, T., Miyake, H., Miura, C., Kamei, H., Aida, K., Miura, T., 2007. Follicle-Stimulating Hormone Induces Spermatogenesis Mediated by Androgen Production in Japanese Eel, Anguilla japonica. Biology of Reproduction 77, 970–977. https://doi.org/10.1095/biolreprod.107.062299.

Pakarainen, T., Zhang, F.-P., Mäkelä, S., Poutanen, M., Huhtaniemi, I., 2005. Testosterone Replacement Therapy Induces Spermatogenesis and Partially Restores Fertility in Luteinizing Hormone Receptor Knockout Mice. Endocrinology 146, 596–606. https://doi.org/10.1210/en.2004-0913.

Park, J.-C., Lee, J.-H., Kodama, K., Urushitani, H., Ohta, Y., Horiguchi, T., 2013. Structure of the intratesticular duct system for sperm emission in the starspotted smooth-hound Mustelus manazo. Fish Sci 79, 203–211. https://doi.org/10.1007/s12562-012-0581-6.

Patel, H., Bhartiya, D., 2016. Testicular Stem Cells Express Follicle-Stimulating Hormone Receptors and Are Directly Modulated by FSH. Reprod. Sci. 23, 1493–1508. https://doi.org/10.1177/1933719116643593.

Piferrer, F.C., Callard, G.V., 1995. Inhibition of Deoxyribonucleic Acid Synthesis during Premeiotic Stages of Spermatogenesis by a Factor from Testis-Associated Lymphomyeloid Tissue in the Dogfish Shark (Squalus Acanthias). Biology of Reproduction 53, 390–398. https://doi.org/10.1095/biolreprod53.2.390.

Planas, J.V., 1995. Maturation-associated changes in the response of the salmon testis to the steroidogenic actions of gonadotropins (GTH I and GTH II) in vitro. Biology of Reproduction 52, 697–704. https://doi.org/10.1095/biolreprod52.3.697.

Prisco, M., Loredana, R., Piero, A., 2002. Ultrastructural studies on developing follicles of the spotted rayTorpedo marmorata. Mol. Reprod. Dev. 61, 78–86. https://doi.org/10.1002/mrd.1133.

Pudney, J., Callard, G.V., 1984. Development of agranular reticulum in Sertoli cells of the testis of the dogfishSqualus acanthias during spermatogenesis. Anat. Rec. 209, 311–321. https://doi.org/10.1002/ar.1092090309.

Quérat, B., Tonnerre-Doncarli, C., Géniès, F., Salmon, C., 2001. Duality of Gonadotropins in Gnathostomes. General and Comparative Endocrinology 124, 308–314. https://doi.org/10.1006/gcen.2001.7715.

Ramaswamy, S., Weinbauer, G.F., 2014. Endocrine control of spermatogenesis: Role of FSH and LH/ testosterone. Spermatogenesis 4, e996025.

Read, T.D., Petit, R.A., Joseph, S.J., Alam, M.T., Weil, M.R., Ahmad, M., Bhimani, R., Vuong, J.S., Haase, C.P., Webb, D.H., Tan, M., Dove, A.D.M., 2017. Draft sequencing and assembly of the genome of the world's largest fish, the whale shark: Rhincodon typus Smith 1828. BMC Genomics 18, 532. https://doi.org/10.1186/s12864-017-3926-9.

Redon, E., Bosseboeuf, A., Rocancourt, C., Da Silva, C., Wincker, P., Mazan, S., Sourdaine, P., 2010. Stage-specific gene expression during spermatogenesis in the dogfish (Scyliorhinus canicula). Reproduction 140, 57–71. https://doi.org/10.1530/REP-10-0021.

Riccetti, L., Yvinec, R., Klett, D., Gallay, N., Combarnous, Y., Reiter, E., Simoni, M., Casarini, L., Akli Ayoub, M., 2017. Human Luteinizing Hormone and Chorionic Gonadotropin Display Biased Agonism at the LH and LH/CG Receptors. Scientific Reports 7, 940. https://doi.org/10.1038/s41598-017-01078-8.

Sambroni, E., Le Gac, F., Breton, B., Lareyre, J.-J., 2007. Functional specificity of the rainbow trout (Oncorhynchus mykiss) gonadotropin receptors as assayed in a mammalian cell line. Journal of Endocrinology 195, 213–228. https://doi.org/10.1677/JOE-06-0122.

Schefe, J.H., Lehmann, K.E., Buschmann, I.R., Unger, T., Funke-Kaiser, H., 2006. Quantitative real-time RT-PCR data analysis: current concepts and the novel "gene expression's C T difference" formula. Journal of Molecular Medicine 84, 901–910. https://doi.org/10.1007/s00109-006-0097-6.

Schwartz, J., Réalis-Doyelle, E., Le Franc, L., Favrel, P., 2021. A Novel Dop2/Invertebrate-Type Dopamine Signaling System Potentially Mediates Stress, Female Reproduction, and Early Development in the Pacific Oyster (Crassostrea gigas). Mar Biotechnol (NY) 23, 683–694. https://doi.org/10.1007/s10126-021-10052-5.

Shayu, D., Rao, A.J., 2006. Expression of functional aromatase in the epididymis: Role of androgens and LH in modulation of expression and activity. Molecular and Cellular Endocrinology 249, 40–50. https://doi.org/10.1016/j.mce.2006.01.016.

Shimoyama, K., Kawano, M., Ogawa, N., Tokunaga, K., Takagi, W., Kobayashi, M., Hyodo, S., 2023. Progesterone initiates tendril formation in the oviducal gland during egg encapsulation in cloudy catshark (Scyliorhinus torazame). Zoological Lett 9, 13. https://doi.org/10.1186/s40851-023-00211-y.

Sievers, F., Wilm, A., Dineen, D., Gibson, T.J., Karplus, K., Li, W., Lopez, R., McWilliam, H., Remmert, M., Söding, J., Thompson, J.D., Higgins, D.G., 2011. Fast, scalable generation of high-quality protein multiple sequence alignments using Clustal Omega. Molecular Systems Biology 7, 539. https://doi.org/10.1038/msb.2011.75.

Sourdaine, P., Garnier, D.H., 1993. Stage-dependent modulation of Sertoli cell steroid production in dogfish (Scyliorhinus canicula). Reproduction 97, 133–142. https://doi.org/10.1530/jrf.0.0970133.

Sourdaine, P., Garnier, D.H., Jégou, B., 1990. The adult dogfish (Scyliorhinus canicula L.) testis: a model to study stage-dependent changes in steroid levels during spermatogenesis. Journal of Endocrinology 127, 451–460. https://doi.org/10.1677/joe.0.1270451.

Stanley, H.P., Kasinsky, H.E., Bols, N.C., 1984. Meiotic chromatin diminution in a vertebrate, the holocephalan fish Hydrolagus collie (Chondrichthyes, Holocephali). Tissue and Cell 16, 203–215. https://doi.org/10.1016/0040-8166(84)90045-4.

Studer, G., Rempfer, C., Waterhouse, A.M., Gumienny, R., Haas, J., Schwede, T., 2020. QMEANDisCo—distance constraints applied on model quality estimation. Bioinformatics 36, 1765–1771. https://doi.org/10.1093/bioinformatics/btz828.

Sudo, S., Kuwabara, Y., Park, J.-I., Hsu, S.Y., Hsueh, A.J.W., 2005. Heterodimeric Fly Glycoprotein Hormone-α2 (GPA2) and Glycoprotein Hormone-β5 (GPB5) Activate Fly Leucine-Rich Repeat-Containing G Protein-Coupled Receptor-1 (DLGR1) and Stimulation of Human Thyrotropin Receptors by Chimeric Fly GPA2 and Human GPB5. Endocrinology 146, 3596–3604. https://doi.org/10.1210/en.2005-0317.

Sumpter, J.P., Dodd, J.M., 1979. The annual reproductive cycle of the female lesser spotted dogfish, *Scyliorhinus canicula* L., and its endocrine control. Journal of Fish Biology 15, 687–695. https://doi.org/10.1111/j.1095-8649.1979.tb03678.x.

Sumpter, J.P., Jenkins, N., Dodd, J.M., 1978. Gonadotrophic Hormone in the Pituitary Gland of the Dogfish (Scyliorhinus canicda L.): Distribution and Physiological Significance. General and Comparative Endocrinology 36, 275–285. https://doi.org/10.1016/0016-6480(78)90034-5.

Suzuki, H., Kazeto, Y., Gen, K., Ozaki, Y., 2020. Functional analysis of recombinant single-chain Japanese eel Fsh and Lh produced in FreeStyle 293-F cell lines: Binding specificities to their receptors and differential efficacy on testicular steroidogenesis. General and Comparative Endocrinology 285, 113241. https://doi.org/10.1016/j.ygcen.2019.113241.

Timossi, C., Ortiz-Elizondo, C., Pineda, D.B., Dias, J.A., Conn, P.M., Ulloa-Aguirre, A., 2004. Functional significance of the BBXXB motif reversed present in the cytoplasmic domains of the human follicle-stimulating hormone receptor. Molecular and Cellular Endocrinology 223, 17–26. https://doi.org/10.1016/j.mce.2004.06.004.

Troispoux, C., Guillou, F., Elalouf, J.-M., Firsov, D., Iacovelli, L., Blasi, A.D., Combarnous, Y., Reiter, E., 1999. Involvement of G protein-coupled receptor kinases and arrestins in desensitization to follicle-stimulating hormone action. Molecular Endocrinology 13. https://doi.org/10.1210/mend.13.9.0342.

Ulloa-Aguirre, A., Zariñán, T., Jardón-Valadez, E., Gutiérrez-Sagal, R., Dias, J.A., 2018. Structure-Function Relationships of the Follicle-Stimulating Hormone Receptor. Front. Endocrinol. 9, 707. https://doi.org/10.3389/fendo.2018.00707.

Van Hiel, M.B., Vandersmissen, H.P., Van Loy, T., Vanden Broeck, J., 2012. An evolutionary comparison of leucine-rich repeat containing G protein-coupled receptors reveals a novel LGR subtype. Peptides 34, 193–200. https://doi.org/10.1016/j.peptides.2011.11.004.

Vassart, G., 2004. A molecular dissection of the glycoprotein hormone receptors. Trends in Biochemical Sciences 29, 119–126. https://doi.org/10.1016/j.tibs.2004.01.006.

Venkatesh, B., Lee, A.P., Ravi, V., Maurya, A.K., Lian, M.M., Swann, J.B., Ohta, Y., Flajnik, M.F., Sutoh, Y., Kasahara, M., Hoon, S., Gangu, V., Roy, S.W., Irimia, M., Korzh, V., Kondrychyn, I., Lim, Z.W., Tay, B.-H., Tohari, S., Kong, K.W., Ho, S., Lorente-Galdos, B., Quilez, J., Marques-Bonet, T., Raney, B.J., Ingham, P.W., Tay, A., Hillier, L.W., Minx, P., Boehm, T., Wilson, R.K., Brenner, S., Warren, W.C., 2014. Elephant shark genome provides unique insights into gnathostome evolution. Nature 505, 174–179. https://doi.org/10.1038/nature12826.

Wang, Q., Arighi, C.N., King, B.L., Polson, S.W., Vincent, J., Chen, C., Huang, H., Kingham, B.F., Page, S.T., Farnum Rendino, M., Thomas, W.K., Udwary, D.W., Wu, C.H., the North East Bioinformatics Collaborative Curation Team, 2012. Community annotation and bioinformatics workforce development in concert - Little Skate Genome Annotation Workshops and Jamborees. Database 2012, bar064. doi: 10.1093/database/bar064.

Wang, P., Liu, S., Yang, Q., Liu, Z., Zhang, S., 2018. Functional Characterization of Thyrostimulin in Amphioxus Suggests an Ancestral Origin of the TH Signaling Pathway. Endocrinology 159, 3536–3548. https://doi.org/10.1210/en.2018-00550.

Wang, J., Liu, Q., Wang, Z., Sheng, X., Zhang, H., Han, Y., Yuan, Z., Weng, Q., 2019. Seasonal expressions of luteinising hormone receptor, follicle-stimulating hormone receptor and prolactin receptor in the epididymis of the male wild ground squirrel (Spermophilus dauricus). Reprod. Fertil. Dev. 31, 735. https://doi.org/10.1071/RD18262.

Waterhouse, A., Bertoni, M., Bienert, S., Studer, G., Tauriello, G., Gumienny, R., Heer, F. T., de Beer, T.A.P., Rempfer, C., Bordoli, L., Lepore, R., Schwede, T., 2018. SWISS-MODEL: homology modelling of protein structures and complexes. Nucleic Acids Research 46, 296–303. https://doi.org/10.1093/nar/gky427.

Wehbi, V., Tranchant, T., Durand, G., Musnier, A., Decourtye, J., Piketty, V., Butnev, V. Y., Bousfield, G.R., Crépieux, P., Maurel, M.-C., Reiter, E., 2010. Partially Deglycosylated Equine LH Preferentially Activates β-Arrestin-Dependent Signaling at the Follicle-Stimulating Hormone Receptor. Molecular Endocrinology 24, 561–573. https://doi.org/10.1210/me.2009-0347.

Xie, Y., Chu, L., Liu, Y., Sham, K.W.Y., Li, J., Cheng, C.H.K., 2017. The highly overlapping actions of Lh signaling and Fsh signaling on zebrafish spermatogenesis. Journal of Endocrinology 234, 233–246. https://doi.org/10.1530/JOE-17-0079.

Ye, J., Coulouris, G., Zaretskaya, I., Cutcutache, I., Rozen, S., Madden, T.L., 2012. Primer-BLAST: A tool to design target-specific primers for polymerase chain reaction. BMC Bioinformatics 13, 1–11. https://doi.org/10.1186/1471-2105-13-134.

Zhang, Z., Lau, S.-W., Zhang, L., Ge, W., 2015. Disruption of Zebrafish Follicle-Stimulating Hormone Receptor (fshr) But Not Luteinizing Hormone Receptor (lhcgr) Gene by TALEN Leads to Failed Follicle Activation in Females Followed by Sexual Reversal to Males. Endocrinology 156, 3747–3762. https://doi.org/10.1210/en.2015-1039.